AD-A153 758 A STUDY OF AERODYNAMIC CONTROL IN STALLED FLIGHT LEADING-EDGE VORTEX FORMATION ANALYSIS(U) ANALYTICAL METHODS INC REDMOND WA J K NATHMAN FEB 85 1/1

UNCLASSIFIED AFWAL-TR-84-3090 F33615-81-C-3626 F/G 20/4 NL

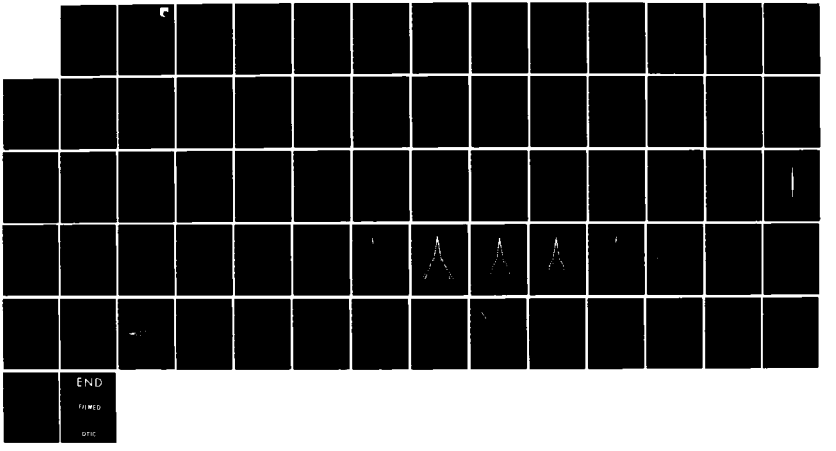

END

FILMED

DTIC

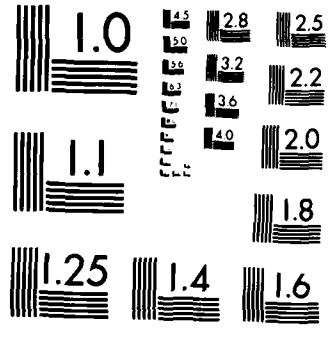

AFWAL-TR-84-3090

A STUDY OF AERODYNAMIC CONTROL IN STALLED FLIGHT
LEADING-EDGE VORTEX FORMATION ANALYSIS

James K. Nathman
ANALYTICAL METHODS, INC.
2047 - 152nd Avenue N.E.
Redmond, Washington 98052

February 1985

Final Report for Period December 1981 - August 1984

FLIGHT DYNAMICS LABORATORY
AIR FORCE WRIGHT AERONAUTICAL LABORATORIES
AIR FORCE SYSTEMS COMMAND
WRIGHT-PATTERSON AIR FORCE BASE, OHIO 45433

NOTICE

When Government drawings, specifications, or other data are used for any purpose other than in connection with a definitely related Government procurement operation, the United States Government thereby incurs no responsibility nor any obligation whatsoever; and the fact that the government may have formulated, furnished, or in any way supplied the said drawings, specifications, or other data, is not to be regarded by implication or otherwise as in any manner licensing the holder or any other person or corporation, or conveying any rights or permission to manufacture use, or sell any patented invention that may in any way be related thereto.

This report has been reviewed by the Office of Public Affairs (ASD/PA) and is releasable to the National Technical Information Service (NTIS). At NTIS, it will be available to the general public, including foreign nations.

This technical report has been reviewed and is approved for publication.

TOM S. WILLIAMS
Project Engineer

VERNON O. HOEHNE
Chief, Control Dynamics Branch
Flight Control Division

FOR THE COMMANDER

FRANK A. SCARPINO
Chief, Flight Control Division

"If your address has changed, if you wish to be removed from our mailing list, or if the addressee is no longer employed by your organization please notify AFWAL/FIGC, W-PAFB, OH 45433 to help us maintain a current mailing list".

Copies of this report should not be returned unless return is required by security considerations, contractual obligations, or notice on a specific document.

Unclassified

SECURITY CLASSIFICATION OF THIS PAGE

REPORT DOCUMENTATION PAGE

1a. REPORT SECURITY CLASSIFICATION: Unclassified	1b. RESTRICTIVE MARKINGS: None
2a. SECURITY CLASSIFICATION AUTHORITY	3. DISTRIBUTION/AVAILABILITY OF REPORT: Approved for public release; distribution unlimited.
2b. DECLASSIFICATION/DOWNGRADING SCHEDULE	
4. PERFORMING ORGANIZATION REPORT NUMBER(S)	5. MONITORING ORGANIZATION REPORT NUMBER(S): AFWAL-TR-84-3090
6a. NAME OF PERFORMING ORGANIZATION: Analytical Methods, Inc. / 6b. OFFICE SYMBOL (If applicable)	7a. NAME OF MONITORING ORGANIZATION: AF Flight Dynamics Laboratory AFWAL (AFSC)
6c. ADDRESS (City, State and ZIP Code): 2047 152nd Ave N.E. Redmond WA 98052	7b. ADDRESS (City, State and ZIP Code): Wright-Patterson AFB OH 45433
8a. NAME OF FUNDING/SPONSORING ORGANIZATION: AFOSR / 8b. OFFICE SYMBOL (If applicable): NA	9. PROCUREMENT INSTRUMENT IDENTIFICATION NUMBER: F33615-81-C-3626
8c. ADDRESS (City, State and ZIP Code): Bolling AFB DC 20332	10. SOURCE OF FUNDING NOS.

PROGRAM ELEMENT NO.	PROJECT NO.	TASK NO.	WORK UNIT NO.
61102F	2307	N3	25

11. TITLE (Include Security Classification): A Study of Aerodynamic Control in Stalled Flight Leading Edge Vortex Formation Analysis

12. PERSONAL AUTHOR(S): Nathman, James K.

13a. TYPE OF REPORT	13b. TIME COVERED	14. DATE OF REPORT (Yr., Mo., Day)	15. PAGE COUNT
Final	FROM Dec 81 TO Aug 84	1985 February	61

16. SUPPLEMENTARY NOTATION

17 COSATI CODES			18. SUBJECT TERMS (Continue on reverse if necessary and identify by block number)
FIELD	GROUP	SUB GR	
01	01		Panel Methods, Unsteady cross-flow analogy, Vortex Sheet
01	02		

19. ABSTRACT (Continue on reverse if necessary and identify by block number)

This report describes the theory and application of VORSEP, a wake preprocessor for panel methods that use an iterative procedure to determine the position of strongly interacting vortex sheets. The estimation of the wake geometry is based on slender body theory with separation. An unsteady, two-dimensional airfoil program was automated with the addition of routines to interpolate cross-sectional geometry from arbitrary three-dimensional bodies, generate multi-core wakes and synthesize a three-dimensional wake structure. Leading-edge wakes for a delta, straked wing and double delta are constructed and used in VSAERO, a three-dimensional panel method. The wake structures compare reasonably well to experimentally observed vortex core positions, while calculated pressures on the wings with the estimated wakes compare well near the nose but less well near the trailing edge.

20. DISTRIBUTION/AVAILABILITY OF ABSTRACT	21. ABSTRACT SECURITY CLASSIFICATION
UNCLASSIFIED/UNLIMITED ☒ SAME AS RPT ☐ DTIC USERS ☐	Unclassified

22a. NAME OF RESPONSIBLE INDIVIDUAL	22b. TELEPHONE NUMBER (Include Area Code)	22c. OFFICE SYMBOL
William B. Blake	513-255-8484	AFWAL/FIGC

DD FORM 1473, 83 APR EDITION OF 1 JAN 73 IS OBSOLETE.

Unclassfied

SECURITY CLASSIFICATION OF THIS PAGE

TABLE OF CONTENTS

LIST OF FIGURES

LIST OF FIGURES (CONCLUDED)

LIST OF SYMBOLS

B	Body surface or potential at control point due to unit normal velocity on boundary
C	Potential at control point due to unit potential on boundary
n	Normal on boundary, s
r	Position vector
s	Boundary of potential domain
v_b	Velocity of the boundary, B
V	Potential domain
V_∞	Flow velocity far from body
W	Wake surface
ϕ	Total potential of flow
θ	Wake merge angle

SUMMARY

This report describes the theory and application of VORSEP, a wake preprocessor for panel methods that use an iterative procedure to determine the position of strongly interacting vortex sheets. The estimation of the wake geometry is based on slender body theory with separation. An unsteady, two-dimensional airfoil program was automated with the addition of routines to interpolate cross-sectional geometry from arbitrary three-dimensional bodies, generate multi-core wakes and synthesize a three-dimensional wake structure. Leading-edge wakes for a delta, straked wing and double delta are constructed and used in VSAERO, a three-dimensional panel method. The wake structures compare reasonably well to experimentally observed vortex core positions, while calculated pressures on the wings with the estimated wakes compare well near the nose but less well near the trailing edge.

1.0 INTRODUCTION

Flow separations are certain to occur on highly swept wings at moderate to high angles of attack. The separations usually produce free vortex layers, joined to the leading edges of the wing, which roll up to form spiral-shaped vortex sheets above the surface, a classical illustration being the vortices over delta wings. These separations lead to important non-linear lift characteristics because both the position and strength of the vortex sheets vary with angle of attack.

The aerodynamic analysis of aircraft with vortex/surface interactions is best handled by panel methods such as VSAERO (Ref. 1) or the Free Vortex Sheet computer code (Ref. 2). These programs use an iterative procedure to determine the position of the vortex sheets. If the initial structure of the vortices is unrealistic, a great deal of computational effort is required for a solution. Indeed, a poor initial structure can lead to an unstable iteration and no solution. A starting solution preprocessor that would decrease the labor involved in generating an initial structure and reduce the iterations necessary for convergence would produce significant cost savings.

Analytical Methods, Inc. (AMI), under Air Force Contract F33615-81-C-3626, is developing such a wake preprocessor for VSAERO. This preprocessor, VORSEP (Refs. 3,4), needs very little additional input above that required for VSAERO, and, for less computational effort than one wake iteration, produces a starting solution for the three-dimensional code. In addition, VORSEP is applicable to very general configurations.

The appendix describes the input file and procedures required to execute VORSEP.

2.0 VORSEP

A flow chart of VORSEP and its relationship to VSAERO is presented in Figure 1. To perform its job as a wake synthesizer for VSAERO, VORSEP

1. determines the body cross-section;

2. distributes the wake starting at the specified separation point, and records the wake shape for VSAERO;

3. solves for the cross-flow around the body; and

4. determines the increase in wake circulation and the wake position for the next time step.

This is repeated for each time step defined by the wake grid planes.

Under Air Force Contract F33615-81-C-3626 AMI has converted an unsteady two-dimensional panel method into a wake preprocessor for VSAERO. This work entailed:

1. establishing the same geometric description of the body for VORSEP as in VSAERO which greatly expands VORSEP's applications;

2. automating the calculation of body cross-section motion;

3. generalizing the specification of the separation line;

4. changing the constant time-step code to a variable spatial marching scheme and allowing a restart capability;

5. adding a multi-core wake model;

6. adding graphic output to VORSEP to ease user interaction; and

7. developing a code to generate from two-dimensional VORSEP output the three-dimensional streamline geometry required by VSAERO.

2.1 Theory

At the heart of VORSEP is an unsteady potential flow code accurate for two-dimensional bodies with separation. It is also applicable to steady, three-dimensional, separated flow over slender bodies. As illustrated in Figure 2, the fluid motion in a plane perpendicular to the x-axis is assumed to be two-dimensional. This two-dimensional cross-flow assumption is commonly used for the roll-up of vortices behind a wing (Refs. 5, 6). In the case of attached flow, the theory has been used by Munk (Ref. 7) and Tsien (Ref. 8) for the lift of a body of revolution and by Jones (Ref. 9) for the flow around low aspect ratio wings for which the solution at one cross-flow plane is independent of other cross-flow planes. Bryson (Ref. 10) added a separated wake in the form of a pair of vortices with feeding sheets to model the flow around circular cylinders and cones. A numerical method for bodies of elliptic (but not constant) cross-section was developed by Schindel (Ref. 11) based on Bryson's theory. Experimental validation of this model is found in References 12 and 13.

In the case of separated flow, the wake is dependent upon the upstream flow history. Variations from one cross-flow plane to the next proceed as if the x-coordinate were time-like in nature. Thus, the theory is referred to as an unsteady cross-flow analogy. VORSEP has been adapted to handle all three cases, a wake without a body, a body without a wake, and bodies with separation.

As noted by Lamb (Ref. 14) and Ashley (Ref. 15), the potential describing an irrotational, incompressible flow can be expressed by its boundary values. This leads to a well-behaved means of solving for the potential, suggested by Morino (Ref. 16). Starting with Laplace's equation, a transform is applied to the differential equation, that is,

$$\int_V \frac{1}{2\pi} \ln|r - r_p| \left\{ \nabla^2 \Phi(r) = 0 \right\} dV \qquad (1)$$

n Green's Theorem it is known that

$$\int_V \frac{\ell n|r - r_p|}{2\pi} \nabla^2\Phi(r)\,dV = \int_V \nabla^2\left(\frac{\ell n|r - r_p|}{2\pi}\right) \Phi(r)\,dV$$

$$+ \int_S \left[\Phi(r) \frac{\partial}{\partial n} \frac{\ell n|r - r_p|}{2\pi}\right.$$

$$\left. - \frac{\partial\Phi}{\partial n} \frac{\ell n|r - r_p|}{2\pi}\right] ds \qquad (2)$$

$$\nabla^2 \left(\frac{\ell n|r - r_p|}{2\pi}\right) = -\delta|r - r_p| \qquad (3)$$

:h δ being the delta function.

Depending upon whether p is inside or outside V the result

$$\int \left[\Phi(r)\frac{\partial}{\partial n}\left(\frac{\ell n|r - r_p|}{2\pi}\right) - \frac{\partial\Phi}{\partial n} \frac{\ell n|r - r_p|}{2\pi}\right] ds = \begin{cases} \Phi(r_p) & p\varepsilon V \quad (a) \\ 0 & p\not\varepsilon V \quad (b) \end{cases} \qquad (4)$$

can be seen immediately from Eq. (4(b)) that no disturbance is
)duced at a point outside the potential region. Thus, a dis-
ibution of singularities according to Green's Theorem on a
ındary of known geometry acts very much like a physical flow
ıside a closed container--any internal flow will produce no
sturbance of the fluid outside the container. The singulari-
:s are not necessarily limited to sources and doublets, but are
:ermined by the Green's function used in Eq. (1).

REFERENCES

"VSAERO, A Computer Program for Predicting the Non-linear Aerodynamic Characteristics of Arbitrary Configurations--Theory Document", To be published as a NASA CR.

Weber, J.A. et al., "A Three-Dimensional Solution of Flows over Wings with Leading-Edge Vortex Separation", AIAA Paper 75-866, Hartford, CT, June 1975.

Maskew, B., "Calculation of Two-Dimensional Vortex-Surface Interference using Panel Methods", NASA CR-159334, December 1980.

Rao, B.M. and Maskew, B., "Flows over Wings with Leading-Edge Vortex Separation", NASA CR-165858, April 1982.

Westwater, F.L., "Rolling Up of the Surface of Discontinuity behind an Aerofoil of Finite Span", Aero. Res. Council, R & M No. 1962, 1935.

Hoejimakers, H.W.M. and Vaatstra, W., "A Higher-Order Panel Method Applied to Vortex Sheet Roll-up", NLR Report MP 81059U; see also AIAA Paper 82.0096 presented at 20th AIAA Aerospace Sciences Meeting, Orlando, Florida, January 1982.

Munk, M.M., "The Aerodynamic Forces on Airship Hulls", NACA Report 184, 1924.

Tsien, H.S., J. Aero. Sci., Vol. 5, 1938, p. 480.

Jones, R.T., "Properties of Low-Aspect Ratio Pointed Wings at Speeds below and above the Speed of Sound", NACA Report 835, 1946.

Bryson, A.E., Jr., "Symmetric Vortex Separation on Circular Cylinders and Cones", J. Appl. Mech., Vol. 26, No. 4, December 1959.

Schindel, L.H., Effect of Vortex Separation on Lifting Bodies of Elliptic Cross Section, M.I.T. Aerophysics Lab., Report TR 118, September 1965.

Friberg, E.G., Measurement of Vortex Separation, Part I: Two-Dimensional Circular and Elliptic Bodies, M.I.T. Aerophysics Lab., Report TR 114, July 1965.

Friberg, E.G., Measurement of Vortex Separation, Part II: Three-Dimensional Circular and Elliptic Bodies, M.I.T. Aerophysics Lab., Report TR 115, August 1965.

Lamb, H., Hydrodynamics, 6th Ed., Dover Publications, New York, N.Y., 1945.

Ashley, H. and Landahl, M., Aerodynamics of Wings and Bodies, Addison-Wesley, Reading, MA, 1965.

4.0 CONCLUSIONS

The extension of an unsteady two-dimensional theory to estimate the wake structure on three-dimensional configurations has been accomplished. The applications included a delta wing, swept wing with strake and double-delta wing. The results indicate that the unsteady cross-flow program, VORSEP, can produce physically realistic wake structures for use in VSAERO. However, the wake circulation calculated by VSAERO for both the swept wing with strake and double-delta wing indicates the method for obtaining the wake strength must be reevaluated in light of the present results. This is not unexpected for the first time VORSEP has been coupled to VSAERO.

The use of a wake model which has no skewed panels and which uses the wake strength calculated by VORSEP gives reasonable correlation with experiment.

The wake structures calculated by VORSEP, particularly those for the double-delta wing, show remarkable fidelity and are certainly an improvement over any initial guess available to the typical VSAERO user.

Finally, the extra data required for the VORSEP calculations is minimal, a sign that savings in labor and computer resources can be achieved.

derneath the vortices where experimental data says the pressure aks. Concentrating the grid planes near the leading-edge kink oduces a marked effect in the pressures, moving them closer to ıe data. Plotting the wake circulation as was done for the ıraked wing, shows that much variation is present in the wake ırength when evenly spaced grid planes are used, Figure 29. The ıcreased wake detail near the leading-edge kink provided by the ıncentrated wake grid planes reduces the scatter and compares ıosely to the VORSEP distribution. The conclusion is that the ılculation of leading-edge wake strength in VSAERO is sensitive ı grid plane placement and guidelines to minimize this effect ıe needed.

Similar effects are also possible from other sources. Two ıssibilities are skewed panels and surface panel density. ıewed wake panels reduce the accuracy of the wake influence ıich is calculated assuming flat panels. Obviously, by concen- ıating the grid planes the panels become smaller and less ıewed. Therefore, one symptom of skewed panels would be a ınsitivity with respect to grid plane placement. The pressures ay also be sensitive to surface panel density because the wake ırength is extrapolated from the surface potential distribution ıd this is better calculated with denser panelling. It was ssumed that 400 panels would represent the double delta ac- ıurately.

Several remedies can be explored. The first that comes to ind is to filter the wake circulation by fitting it to a low- rder curve as done by Rao and Nathman (Ref. 28). This prevents he occurrence of vortices of the wrong sign and improves wake elaxation. Another possibility is not to calculate the circula- ion, but to apply the circulation from VORSEP. In other words, reat the wake strength as a known quantity instead of an un- nown. Inaccuracy caused by skewed panels is expected to be vercome by adopting a calculation that is exact for non-flat anels. AMI is currently developing a version of VSAERO with a ake grid limit greater than 31.

Essentially all of the above procedures were used to deter- ine the most favorable outcome from VSAERO. The VORSEP wake was implified to a model much like that of Brown and Michael (Ref. 9), which eliminated skewed wake panels and the sensitivity to ake grid planes. The wake is shown in Figure 30. Further, the ORSEP circulation was supplied to VSAERO, thus circumventing ifficulties in applying a Kutta condition at the leading edge. he result is shown in Figure 31. The correlation between theory nd experiment is now markedly better than in Figure 27. A ignificant pressure rise appears under the primary vortex and he pressure decreases outboard of the secondary vortex.

vortices join upstream toward the leading edge kink. Quantitatively, Hummel observed that the vortex joining occurs at the trailing edge at 11° and occurs at the leading-edge kink by 20°. VORSEP predicts angles of attack of 13° and 26°, respectively, a difference of 30%. If the position of the vortex axes as observed by Hummel at 12° is compared to the prediction of VORSEP at 15° (30% higher than experiment), a very good correlation is obtained as seen in Figure 23. The VORSEP strake vortex is slightly outboard of the experimental position, but the vortex from the leading-edge kink follows the observed position closely.

An interesting point here is that in the study of a swept wing with strake it was shown that the wake geometry was very sensitive to the sharpness of the leading edge. In that study VORSEP compared best at an angle of attack 30% lower than the experimental results. The conclusion is that leading-edge geometry effects which are not fully accounted for in VORSEP can lead to the discrepancies seen.

Figure 24 shows a cross section of the wake over the Hummel wing. The experimental data shows the vortex sheet and contours of constant total pressure which peak at vortex cores. Superimposed on the observed data are the vortex core positions and wake sheets from VORSEP. The amalgamation procedure produces the gap between the two wake sheets.

Again, the experimental angle of attack is 12°, while the VORSEP geometry is for 15°. Nevertheless, it is obvious that VORSEP reproduces the wake structure very well. The inboard vortex lies within a few percent of local span of its observed position. The outboard vortex is significantly further outboard, but it is very close to the right height above the wing. Also the vortex sheet, particularly as it leaves the leading edge, lies quite close to the observed position.

The calculated wake structures were used in VSAERO at angles of attack of 10°, 12° and 15°. The solution at 10° for which there is no experimental comparison shows the expected single pressure peak over the forward delta, Figure 25, and a double-peaked spanwise velocity caused by the two separate vortices over the main wing, Figure 26. At 12° and 15°, for which Hummel has published pressure data for a cross section at 75% chord, the comparison between VSAERO and data is not good, Figures 27 and 28. Two sets of results from VSAERO are presented--one for equally spaced wake grid planes, and the other for grid planes concentrated near the leading-edge kink.

The wake panels in VSAERO are defined by the intersection of the wake streamlines and the wake grid planes, which need not be the same as those used in VORSEP. In both cases at 12° angle of attack, the streamline geometry was the same, and was produced by VORSEP in one run. So the only difference is the distribution of wake panels since the VSAERO limit of 31 grid planes was used. For equally spaced grid planes, the pressure distribution is flat

the wing. However, over the main wing the circulation is markedly higher than that calculated by VORSEP.

Slightly better agreement would be obtained if only the streamwise circulation in VSAERO were plotted, but the 15% difference would not substantially decrease the strength of the wing vortex which, near the strake/wing juncture, is twice that predicted by VORSEP. Reducing the vorticity (the slope of the circulation curve) would reduce the wing vortex strength, and, hence, the pressures under the core, leading to better correlation between VSAERO and experiment.

3.3 Double-delta Wing

VORSEP with the new multi-core wake was applied to the double delta wing planform VI tested by Hummel (Ref. 22). This wing is one of several for which surface pressures, streamlines and wake total head were measured. Wing VI has a kink in the leading edge at one-half of the root chord. The forward delta or strake has a leading-edge sweep of 80°. The rear delta is swept 70°. The airfoil was a flat plate with a thickness of 0.6% root chord. The leading edges were semicircles.

Wake structures over the wing were constructed for angles of attack of 10°, 12°, 15° and 20°. These are shown in Figures 19 through 22. The wake at 10° in Figure 19 was constructed with two wake models: one for the strake leading edge, and one for the wing leading edge. For low angles of attack where there is little interaction between the strake and wing cores, this is an accurate representation. For the higher angles, the multi-core wake model was used to allow for more intense interaction of the cores. Each analysis required about 200 time steps from the starting point at 10% root chord to the trailing edge.

It should be pointed out here that the calculations must start downstream of the apex where conical flow would require an infinitesimal time step. (It would be possible to adapt the conical flow program of Schindel (Ref. 11) to generate a starting solution, and indeed, a single vortex like Bryson's of the correct strength and position has been used to minimize the transient disturbances in the core position.) However, the disturbances produced by starting at 10% of the root chord quickly die out and it will be seen in all the figures that the strake vortex core can be extrapolated forward to the apex exactly as if it had originated there.

The qualitative behavior of the core trajectories follows that of experiment. That is, beginning at the lowest angles of attack, Figure 19, two distinct vortices are present. As the angle of attack increases, the strake vortex moves outboard until it joins with the wing vortex at the trailing edge, Figure 21. Further increases in angle of attack move the point at which the

At low angles of attack the vorticity shed by the strake and wing rolls up into two distinct vortex cores. At higher angles of attack when the vortices are stronger, these two cores intertwine just downstream of the strake/wing juncture, forming one vortex core. This behavior is influenced not only by the angle of attack but also by the leading-edge shape which affects the amount of vorticity shed into the wake. Experimental observations at the same angle of attack show that the vortices over the sharp-edged configuration 6 intertwine at much lower angles of attack.

If the wake is modelled with one wake in VORSEP, then the resulting structure at an angle of attack of 20° is biased towards combining all the vorticity into one core. The path of the vortex core, shown in Figure 15, is not unlike that seen over configuration 6.

If we decide to allow more detail in the wing wake by modelling it as a second wake in VORSEP, Figure 16, then the wake structure appears more like that found on configuration 3A. In fact, it appears remarkably close to the wake found at a slightly higher angle of attack, 26°. The six degree deviation is not surprising in view of the sensitivity of the wake structure to small variations in geometry. If less vorticity had been shed into the wake, the strake vortex would remain separate from the wing vortex.

The second wake structure was chosen to couple VORSEP with VSAERO. The pressure distributions predicted by VSAERO at 10 and 50% local wing chord are shown in Figure 17. At 10% local chord, the predicted pressure distribution agrees very well with experiment in the position of the pressure peaks under the strake and wing vortices. The prediction is markedly higher under the wing vortex. At 50% chord, the prediction continues to show a separate pressure peak under the strake vortex as does experiment, but qualitatively the pressures are too high. Also, the leading-edge pressures indicate the flow is not leaving the wing smoothly. Closer to the trailing edge predicted pressures are higher than experiment. Besides the fact that the predicted vortex will be too low as in the case of the delta wing, the trailing-edge loading under the wing vortex is high because the trailing vorticity streams straight back instead of flowing spanwise under the influence of the leading-edge vortex. This violation of the Kutta condition has been observed by other researchers (Ref. 28). Once the trailing-edge wake is relaxed this peak should be reduced.

Figure 18 plots the wake circulation as a function of wing root chord. This is compared to the circulation calculated by VORSEP. It is apparent that over the strake, where the low-aspect ratio assumption of VORSEP is observed, VSAERO agrees remarkably closely with VORSEP. This is true even if the wake in VSAERO is from the strake only and attached flow is assumed over

3.0 APPLICATIONS

3.1 Delta Wing

When applied to a unit aspect-ratio delta wing at 20° angle of attack, VORSEP generates the smooth wake spiral shown in Figure 10. If we compare the position of the vortex core to experimental measurement (Ref. 19), we find that its vertical position, Figure 11, is predicted well by VORSEP. For a conical geometry, VORSEP will show a nearly linear increase in height with distance downstream; any non-linearity is due to the amalgamation scheme and initial transients from starting at a finite distance from the apex. In this case, where the wing has a biconvex airfoil section, the vortex height tends to increase more rapidly near the nose, and less so near the trailing edge. The discrepancy between VORSEP and experiment at the trailing edge is mainly due to the three-dimensional quality of the flow in which the core begins to parallel the free stream as it approaches the trailing edge. In plan view, Figure 12, the predictions are markedly more outboard than the experiment.

Using the aforementioned wake tracking scheme, the trajectories of the wake filaments attached to the leading edge were constructed and shown in Figure 13. It should be noted that all the filaments are well behaved in that they leave the leading edge at approximately the same angle and wind about the core evenly. The noticeable kinks in each filament occur at the grid planes which divide each wake strip into panels.

The pressure distributions obtained from VSAERO are shown in Figure 14. The upper surface distribution at 30% of root chord compares favorably to Smith's (Ref. 26) conical flow theory or experiment inboard of the secondary separation line. The other upper surface pressure peaks are too narrow and are further outboard than experiment. The lower surface pressures at 70 and 90% root chord do not approach the upper surface pressures at the leading edge but behave somewhat like the pressures found in attached flow.

3.2 Swept Wing with Strake

To investigate the utility of VORSEP for a more complex planform, wake structures were generated over a swept wing with strake. The wing modelled was used by White et al. (Ref. 27) in wind tunnel tests during an investigation of vortex flow control for high-lift generation. Basically, the wing is made of a sharp-edged strake with 75° leading-edge sweep attached to a tapered wing with 50° leading-edge sweep. During the experiment various devices were attached to the wing including a separator plate which changed the rounded leading edge of configuration 3A into the sharp edge of configuration 6.

The doublet strength does not always vary monotonically along the arc of the wake. In such a case, the position of a particle as a function of the doublet strength becomes multi-valued for some doublet values. This can lead to more than one point from which to choose. The solution to this problem is to remember which wake panel the particle was on in the previous time step and select the point closest to that panel.

For the wakes considered so far, this has proven a reliable and economical means of generating three-dimensional streamline trajectories.

extent of the wake is measured. As in the single core model, vortices are accumulated by the secondary core if they wind too far about the core.

2.5 Streamline Tracker

VORSEP redistributes the free vorticity to stabilize the calculation of wake motion. This complements the capability of panelling the body at each time step according to the instantaneous needs required by body and wake geometry. However, the redistribution destroys any connection between an individual vortex (the edge of a wake panel) and the position of a particle attached to the wake. The path of such a particle will be a streamline in the three-dimensional flow; in particular, it is the trajectory of a continuous wake vortex.

To track the trajectory of a streamline, it is conceivable to release imaginary particles from the desired starting points and follow their positions in space. It is preferable to use the velocities at nearby wake vortices instead of calculating the velocities at the particles because velocity calculations are expensive, and, since the particles are dispersed arbitrarily among the wake vortices, their velocities cannot be calculated accurately by direct application of the Biot-Savart law.

A method which avoids expensive velocity calculations and also obviates storing the position of imaginary particles was developed for VORSEP. This method uses the invariance of the doublet strength along a wake streamline to track the streamline trajectory. Referring to Figure 8, we see the vortex sheet shapes produced by VORSEP at four time steps over the tip of a swept wing. For each vortex sheet we can plot the value of the doublet strength of the sheet against the arc length, starting at the separation point, as in Figure 9. If the vorticity shed into the wake has always been of the same sign, the doublet strength will decrease monotonically from its value at the separation point to zero at the end of the wake sheet. The doublet strength at the separation point also grows monotonically with each time step.

To find the corresponding positions (S2, S3) at two time steps (t2, t3) on a streamline it is only necessary to find the points with equal doublet strength. This doublet strength is the same at every time step and is the doublet strength at the separation point at the time the particle left the body. To begin tracking a streamline, VORSEP requires only the station at which the streamline originates. When that station is passed, VORSEP interpolates between the time steps which bracket the starting station for the doublet strength at the separation point. This is stored and the corresponding point at each succeeding time step is readily interpolated from the known doublet strength distribution on the wake.

The wake model developed for VORSEP is quite similar to that in the Free Vortex Sheet computer code. As seen in Figure 6, it consists of a free vortex sheet, modelled by doublet panels, and a vortex core which is an amalgamation of all the free vorticity that has passed a user-controlled merge angle. A feeding sheet connects the free vortex sheet and the core. At each time step the free vorticity is distributed at evenly spaced intervals over the free sheet. This redistribution, similar to that of Fink and Soh (Ref. 19), stabilizes the motion of the wake. As a result, no stability problems have appeared in the time spans necessary to reach the trailing edge. Indeed, calculations have also proceeded beyond the trailing edge of several wings.

The increased circulation shed onto the wake is determined by the condition

$$\Delta\Gamma_w|_{sep} = \int \tfrac{1}{2}\left[\frac{\partial q}{\partial s}\right]^2 dt \qquad (12)$$

where $\frac{\partial q}{\partial s}$ is the surface velocity at the separation point. This follows the work of Clements (Ref. 20) and Smith (Ref. 21).

Each wake model had, until recently, only one core. Multiple vortex cores were modelled with separate wakes which could interact only weakly. A multi-core wake model was added to analyze double-delta wings. VORSEP has the capacity to include up to four wakes simultaneously.

2.4 Multi-core Wake Model

The kink in the leading-edge of a double delta wing causes a rapid increase in shed circulation which rolls up into a vortex core separate from that shed from the more highly swept strake. At low angles of attack the two vortex cores from strake and wing remain separate but at higher angles they intertwine. This process is well documented in References 22 and 23.

From an earlier study (Ref. 24) on a swept wing with strake it was found that modelling the strake and wing separation with one wake in VORSEP biased the solution towards amalgamating both cores into one. If the separation was modelled with two wakes, the interaction between the two cores was either weak or catastrophic. Because the behavior of the two vortex cores over the Hummel double delta wing plays an important role in its aerodynamics, a multi-core wake model was developed.

This wake model, illustrated in Figure 7, is a progressive extension of the single core model, Figure 6. At some point along the separation line, the user prescribes the origin of the secondary core. The vortex leaving the separation line at that point becomes another reference point about which the angular

occurs. Also since this is a parabolic code and only the wake geometry and strength is required to continue the calculation, a restart capability has been added. Should the solution become disturbed for any reason, it is only necessary to back up to the last valid time-step and restart execution. Graphics routines for quickly appraising the wake geometry in the cross-flow plane and the synthesized three dimensional wake have been developed.

2.3 Wake Model

The choice of a wake model for computing the roll-up of a vortex sheet has three objectives. One is to neutralize the inherent instability often encountered by an arbitrary, infinitely thin shear layer (see Moore, Ref. 17). This mathematical instability produces a chaotic motion regardless of the detail of the wake structure. Judicious modifications to the model, such as minimum vortex spacing (or panel size for higher-order methods (Ref. 6)), and viscous core vortices (Ref. 18), can dampen the instability to an acceptable level. The second objective is to suppress small-scale structures that have no significant effect on the flow but require extensive computational effort. An example of this is the modelling of the core of a wing tip vortex. The infinite-spiral vortex sheet can be modelled to the limit allowed by the particular computer but a point is very quickly reached where viscous effects dominate in the real flow, making the idealized structure only of academic interest. Vortex amalgamation is a well known technique for eliminating small-scale structures. The final reason for selecting a wake model is economy. This is especially important to VORSEP, which is intended to be a less expensive means of calculating a wake shape than three-dimensional wake relaxation in VSAERO. Some accuracy can be sacrificed for economy because the accuracy of the two-dimensional calculation is a moot question once the shape has been changed by VSAERO, and because wake roll-up, especially over a solid surface, is a three-dimensional process that can only be approximated by unsteady, two-dimensional calculations.

The fact that VORSEP is linked to VSAERO also bears on the first two points. Whether a wake model is ultimately unstable may be of little consequence to VORSEP if the instability affects only the wake structure far from the body. This determines what is an acceptable level for the instability. The three-dimensional model used in VSAERO is also limited in the amount of detail which can be included in the body and wake geometry, a limit that is far below the specifics VORSEP can generate. Therefore, it makes little sense for VORSEP to faithfully model the spiral shape of a wake produced by a strake or snag and then replace that spiral with a single vortex in the three-dimensional model.

Effort on improving the proficiency of VORSEP in handling geometry has centered on a routine called SLICE. The motivation for developing SLICE is to simplify the input to VORSEP by exploiting the powerful geometry routines in VSAERO and at the same time to establish a way of describing an aircraft geometrically which can be common to both VORSEP and VSAERO.

SLICE generates two-dimensional section cuts from three-dimensional geometry files. For example, SLICE generates cross-sections when given the panel corner points of the fuselage. The three-dimensional information which SLICE expects is the corner point coordinates of the panels that compose the configuration. This is contained in the geometry files produced by VSAERO, so no development is required to produce these files. The geometry routines in VSAERO can panel very complex aircraft with minimal input.

SLICE provides VORSEP with two-dimensional geometry, including the number of bodies in the section, their apparent motion (source strengths) and the positions of separation points based upon simplified user input. One advantage of having access to a three-dimensional geometry file compared to the former station data shows up in computing the source strengths. The three-dimensional panel normals indicate the instantaneous rates of growth. That is, the apparent velocity of the body cross section is

$$v_b \cdot n = \frac{n_x}{\sqrt{1 - n_x^2}} \qquad (11)$$

where n_x is the component of the surface normal perpendicular to the cross-flow plane. This method of calculating body motion is simpler than inferring growth from the differences in geometry at two stations. The latter method required the two-dimensional panelling be the same at all stations, whereas SLICE is allowed to panel each section in an optimum manner.

As an example of its capabilities, the STOL fighter shown in Figure 5 was analysed. A station cut at x=100 shows the sharp-edged strakes at which separation is expected. In this output from SLICE, the three-dimensional flat panels are apparent. When VORSEP produces two-dimensional panelling using SLICE's output, the dense subpanelling results in smooth surfaces for the canopy and belly. This figure demonstrates the ability of SLICE and VORSEP to handle multiple bodies at a time.

Other improvements made to VORSEP to increase its generality include: specification of the separation line as an arbitrary curve on the body surface instead of associating it with the panelling; and a variable time-step capability which decreases the execution time compared to the old fixed time-step. Variable time-steps are particularly useful when any rapid transient, such as the initiation of a wake or a kink in the separation line,

These observations result in the equation

$$\tfrac{1}{2}\Phi(r_p) = \int_B \left[\Phi(r)\ \frac{1}{2\pi}\ \frac{\partial}{\partial n}\ \ell n|r - r_p| - \frac{\partial \Phi}{\partial n}\ \frac{1}{2\pi}\ \ell n|r - r_p|\right] ds$$

$$+ \int_W \Delta\Phi(r)\ \frac{1}{2\pi}\ \frac{\partial}{\partial n}\ \ell n|r - r_p|\, ds + V_\infty \cdot r_p \qquad (8)$$

This is an integral equation for the surface potential given the tangent flow boundary condition on the body

$$\frac{\partial \Phi}{\partial n}\ (r) = v_b \cdot n \qquad (9)$$

where v_b is the velocity of the body surface. Note that for internal flows (inside ducts, wind tunnels, etc.) where Eq. (7) cannot be applied, the only boundary condition is the Neumann boundary condition, Eq. (9). The resulting Neumann problem admits an arbitrary constant potential as a solution. Further, no solution exists unless the integrated normal velocity is zero.

Discretization of the integral equation results in the matrix equation

$$[C]\{\Phi\} = [B]\{\frac{\partial \Phi}{\partial n}\} + \{V_\infty \cdot r\} + [C_w]\{\Delta\Phi_w\} \qquad (10)$$

where only known quantities appear on the right hand side. The wake potential distribution, $\Delta\Phi_w$, is known from the previous time step.

2.2 Panel Method

The above theory was programmed into a code originally developed by Maskew (Ref. 4). In this program, as seen in Figure 4, biquadratic interpolation of the coordinates generates a smooth, dense set of subpanels to represent the surface between points of discontinuous slope on the cross section. The potential and its normal derivative are constant on each subpanel. Finally, an odd number of adjacent subpanels (3 for these results) are grouped into one panel with a biquadratic variation of potential assumed over adjacent panels, thus reducing the number of unknowns by a factor of three.

Regardless of whether the point p approaches the surface from inside V or outside V, the resulting equation is

$$\tfrac{1}{2}\Phi(r_p) = \int_S \left[\Phi(r)\ \frac{1}{2\pi}\ \frac{\partial}{\partial n}\ \ell n|r - r_p|\right.$$

$$\left. - \frac{\partial \Phi}{\partial n}\ \frac{1}{2\pi}\ \ell n|r - r_p|\right] ds \qquad (5)$$

The surface integral now neglects the small neighborhood around p in which the kernel, $\frac{\partial}{\partial n}\left(\frac{\ell n|r - r_p|}{2\pi}\right)$, is singular. The contribution from this part of the integral is $\tfrac{1}{2}\Phi(r_p)$ if p approaches from inside V and $-\tfrac{1}{2}\Phi(r_p)$ if p approaches from outside V.

For our particular problem the boundary, S, extends over the body, B, its wake, W, and out to a contour at infinity, Σ, as shown in Figure 3.

Several observations allow Eq. (5) to be simplified. The first is that on the upper and lower side of the thin wake the normal derivatives are equal and opposite, i.e.,

$$\left.\frac{\partial \Phi}{\partial n}\right|_{\text{upper}} = - \left.\frac{\partial \Phi}{\partial n}\right|_{\text{lower}} \qquad (6)$$

so that only the potential difference, $\Delta\Phi = \Phi_{\text{upper}} - \Phi_{\text{lower}}$, need be considered on the wake, W. The contribution from the contour at infinity can be determined by the requirement for uniform flow; namely,

$$\Phi(r) \to V_\infty \cdot r \qquad \text{as } r \to \infty \qquad (7)$$

16. Morino, L., "Unsteady Compressible Potential Flow around Lifting Bodies Having Arbitrary Shapes and Motions", TR-72-01, Boston University, June 1972.

17. Moore, D.W., "A Numerical Study of the Roll-up of a Finite Vortex Sheet", J Fluid Mech., Vol. 63, Part 2, 1974, pp. 224-235.

18. Chorin, A.J. and Bernard, P.S.,"Discretization of a Vortex Sheet with an Example of Roll-up", FM-72-5, College of Engr., Univ. of California, Berkeley, CA, November 1972.

19. Fink, P.T. and Soh, W.K., "A New Approach to Roll-up Calculations of Vortex Sheets", Proc. Royal Soc. of London, Series A, Vol. 362, 1978, pp. 195-209.,

20. Clements, R.R., "An Inviscid Model of Two-Dimensional Vortex Shedding", J. Fluid Mech., Vol. 57, Part 2, 1973, pp. 321-336.

21. Smith, J.H.B., "Inviscid Fluid Models Based on Rolled-up Vortex Sheets for Three-Dimensional Separation at High Reynolds Number", AGARD LS 94, (Three-Dimensional and Unsteady Separation at High Reynolds Numbers), May 1978.

22. Brennenstuhl, U. and Hummel, D., "Vortex Formation over Double-Delta Wings", ICAS Paper 82-6.6.3, 1982.

23. Nathman, J.K., Norton, D.J. and Rao, B.M., "An Experimental Investigation of Incompressible Flow over Delta and Double-Delta Wings", Office of Naval Research, Report ONR-CR215-231-3, December 1976.

24. Nathman, J.K., "Estimation of Wake Roll-up over Swept Wings", 2nd Applied Aerodynamic Conference, Paper AIAA 84-2174, August 1984.

25. Hummel, D., "Study of the Flow around Sharp-Edged Slender Delta Wings with Large Angles of Attack", NASA Tech. Translation, NASA TT F-15, 107.

26. Smith, J.H.B., "Improved Calculations of Leading-Edge Separation from Slender, Thin, Delta Wings", Proc. Roy. Soc., London, Ser. A., 306, 1968, pp. 67-90.

27. White, R.P., Gangwani, S.T. and Balcerak, J.C., "A Theoretical and Experimental Investigation of Vortex Flow Control for High Lift Generation", Office of Naval Research Report ONR-CR-212-223-3, December 1976.

28. Rao, B.M. and Nathman, J.K., "Analytical and Experimental Investigations of Delta Wings in Incompressible Flow", Office of Naval Research Report ONR-CR215-321-2, December 1976.

29. Brown, C.E. and Michael, W.H., "On Slender Delta Wings with Leading-Edge Separation", NACA TN 3430, 1955.

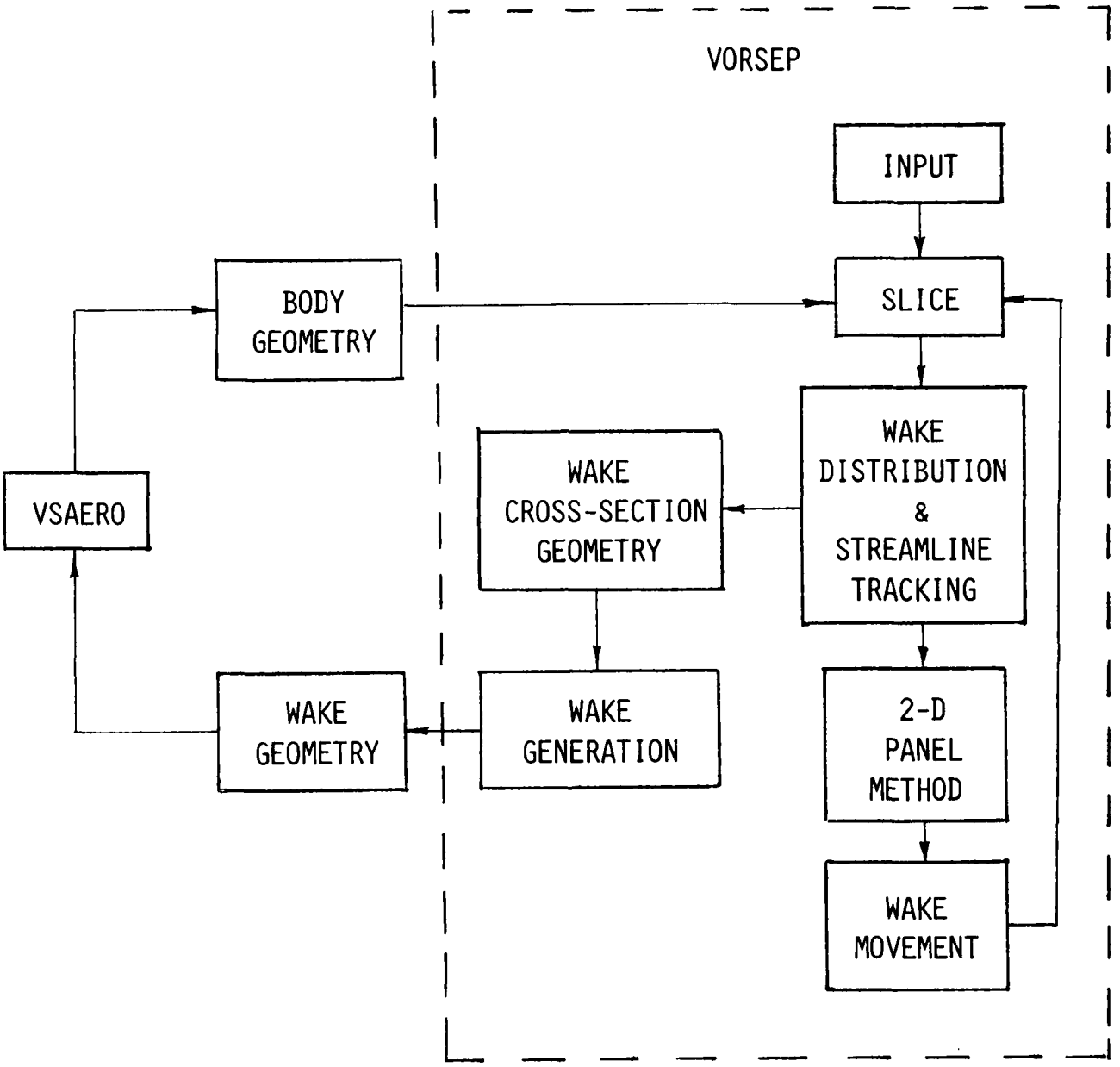

Figure 1. VORSEP Flow Chart

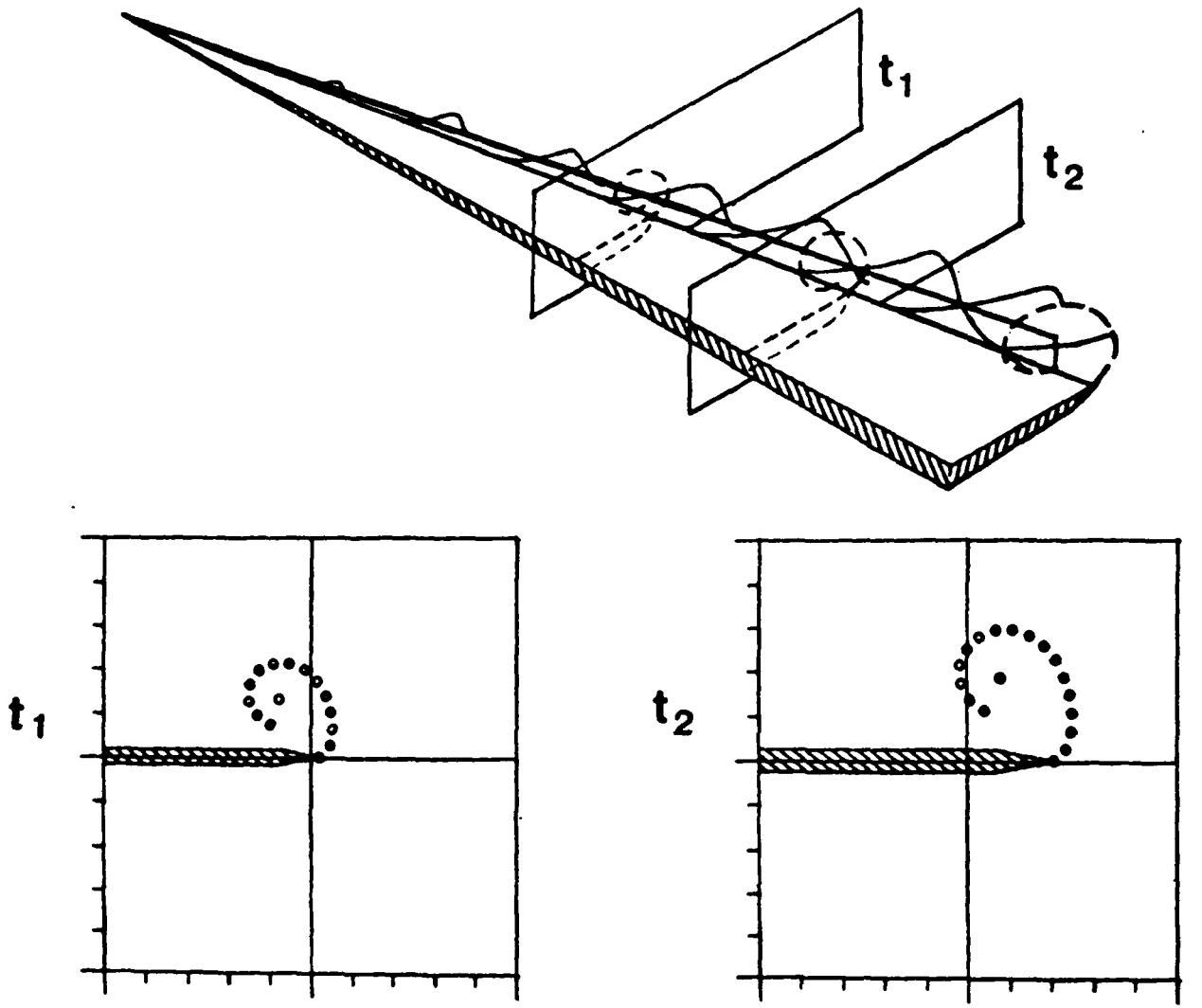

Figure 2. Unsteady Cross-Flow Analogy.

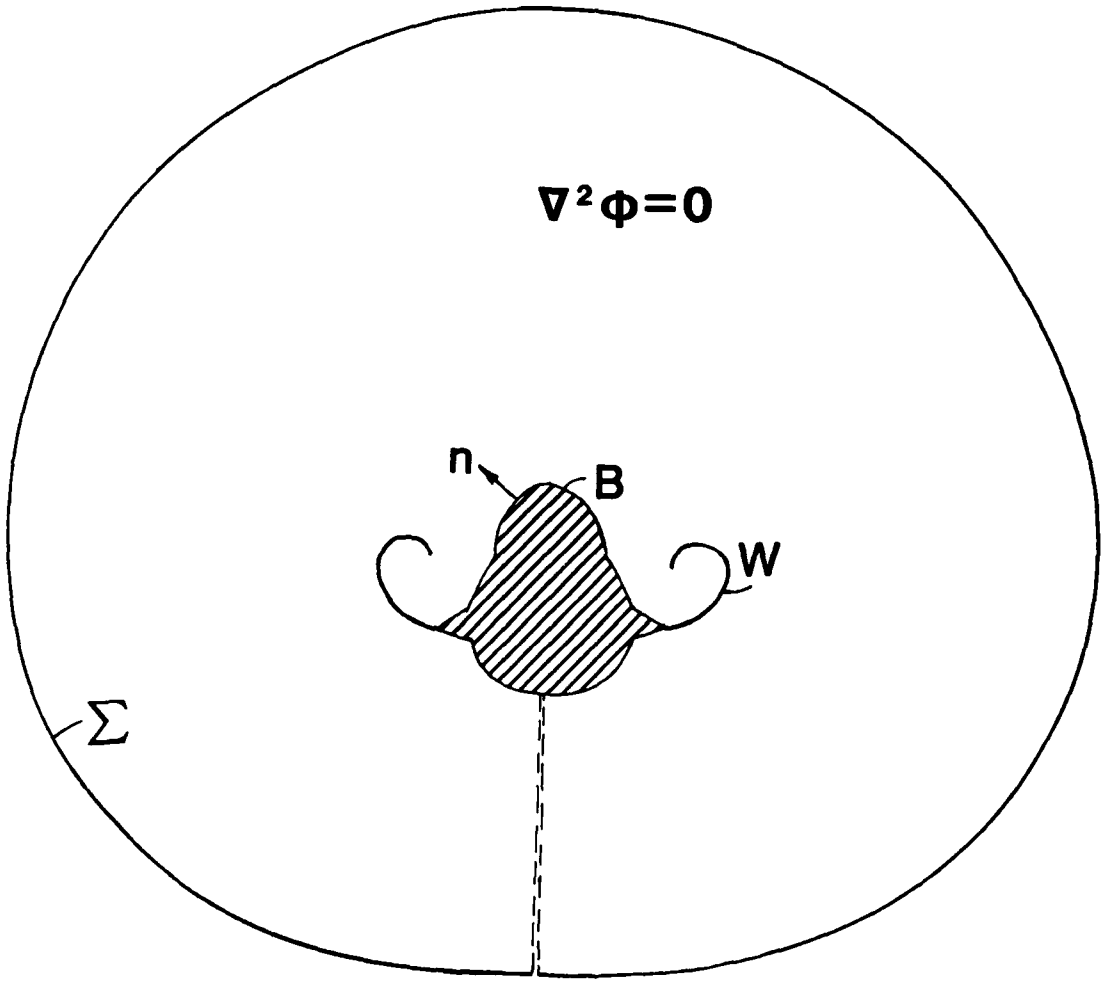

Figure 3. Potential Flow Domain.

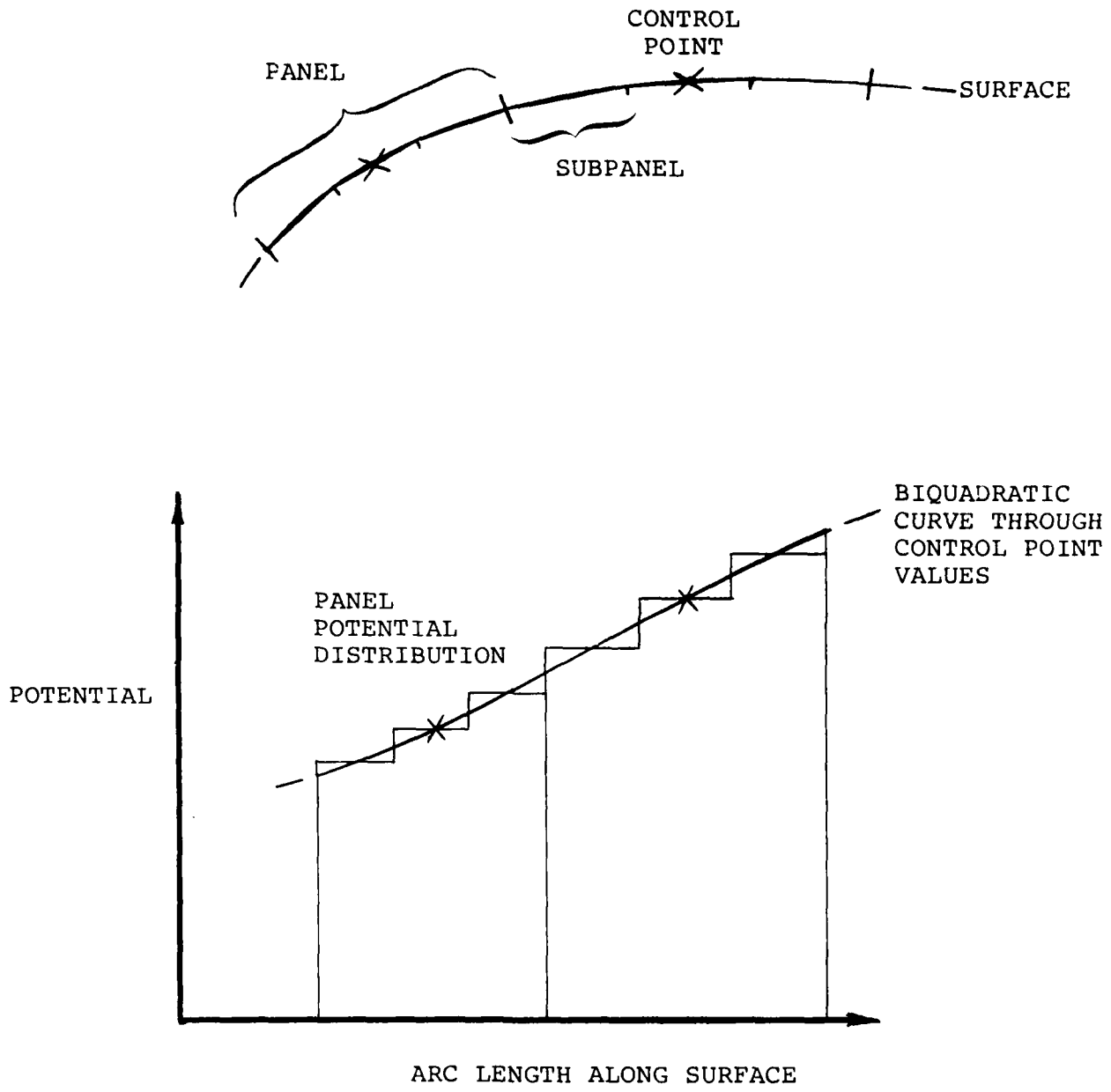

Figure 4. Theoretical Surface Panelling and Potential Distribution.

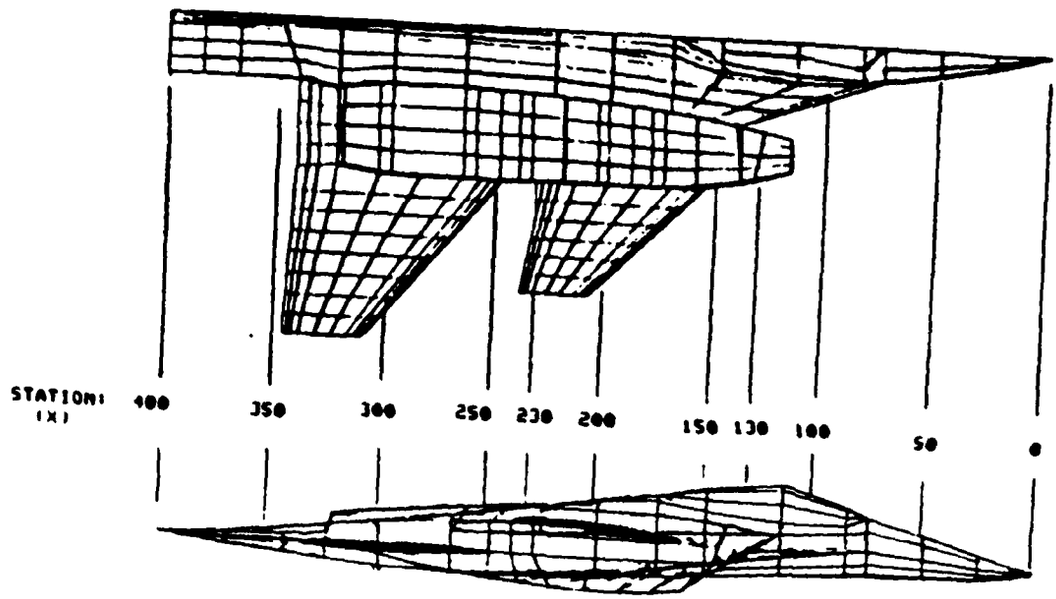

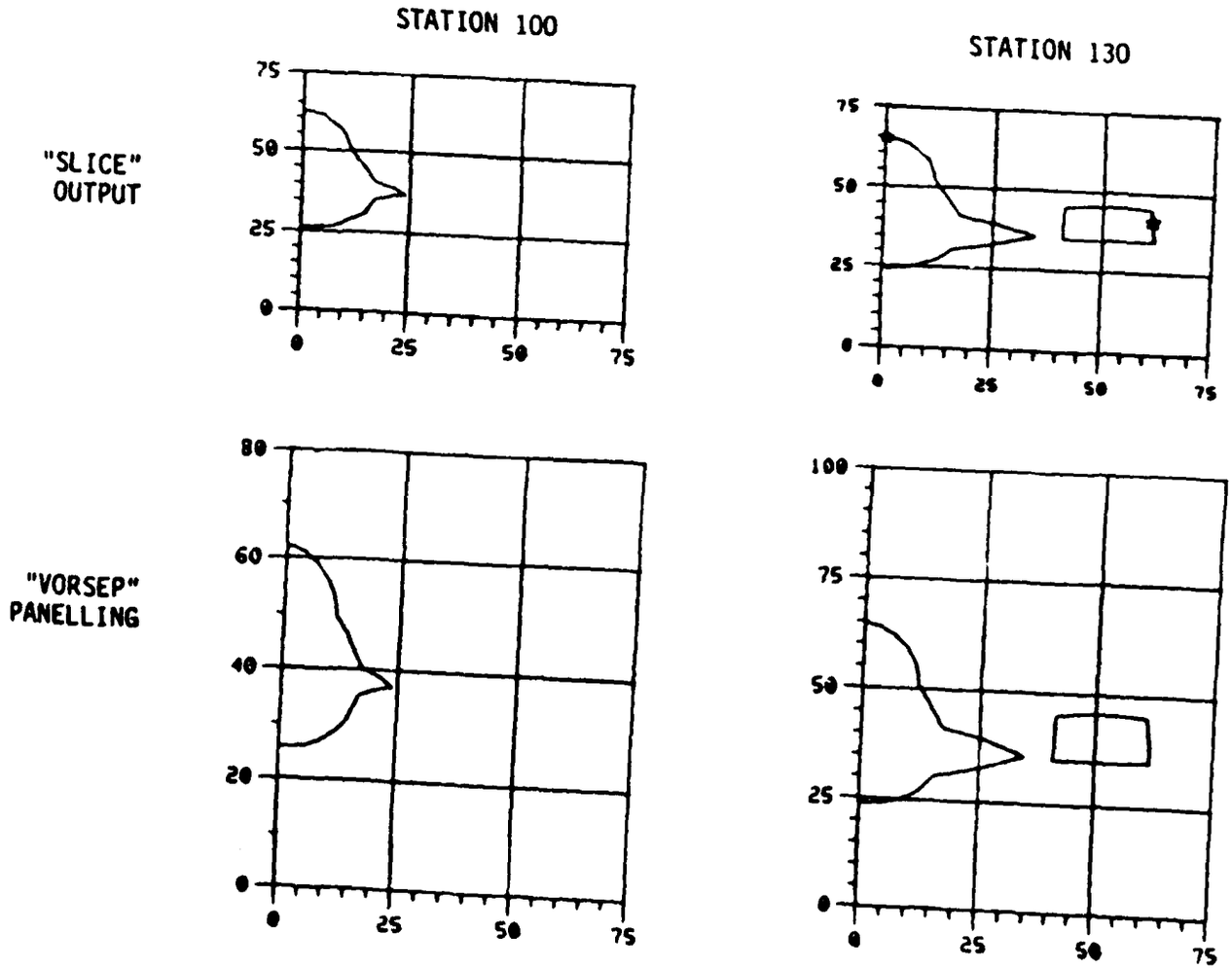

Figure 5. Complex Geometric Capability of VORSEP.

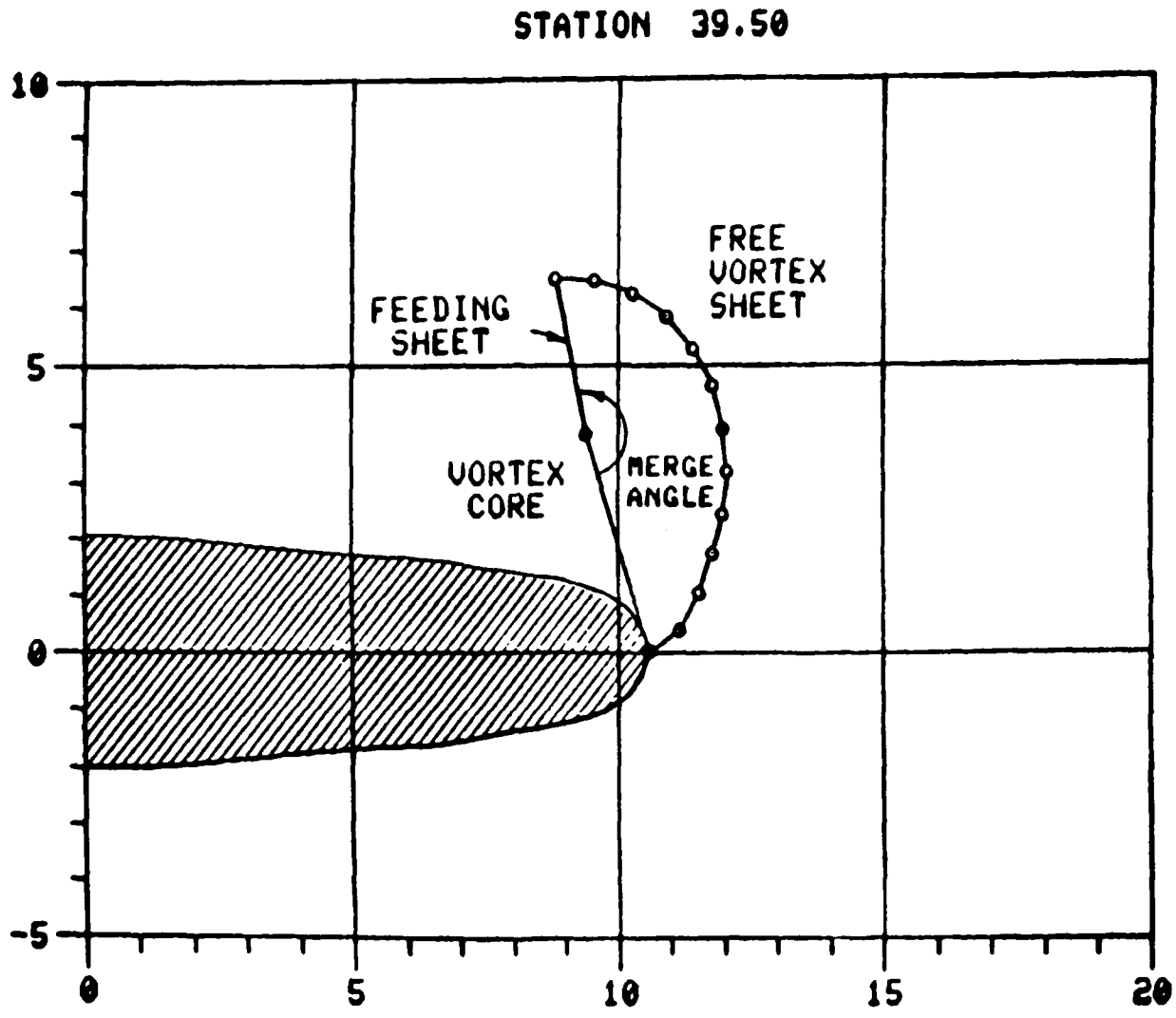

Figure 6. VORSEP Wake Model.

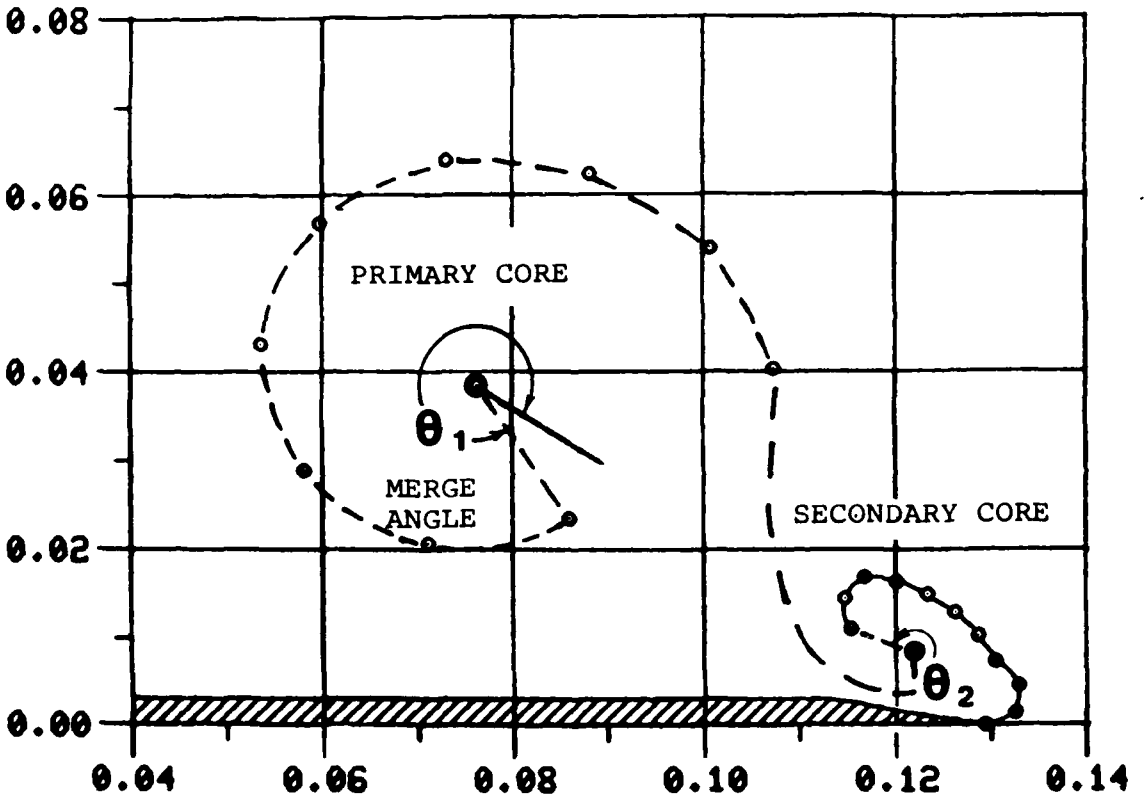

Figure 7. Multi-Core Wake Model.

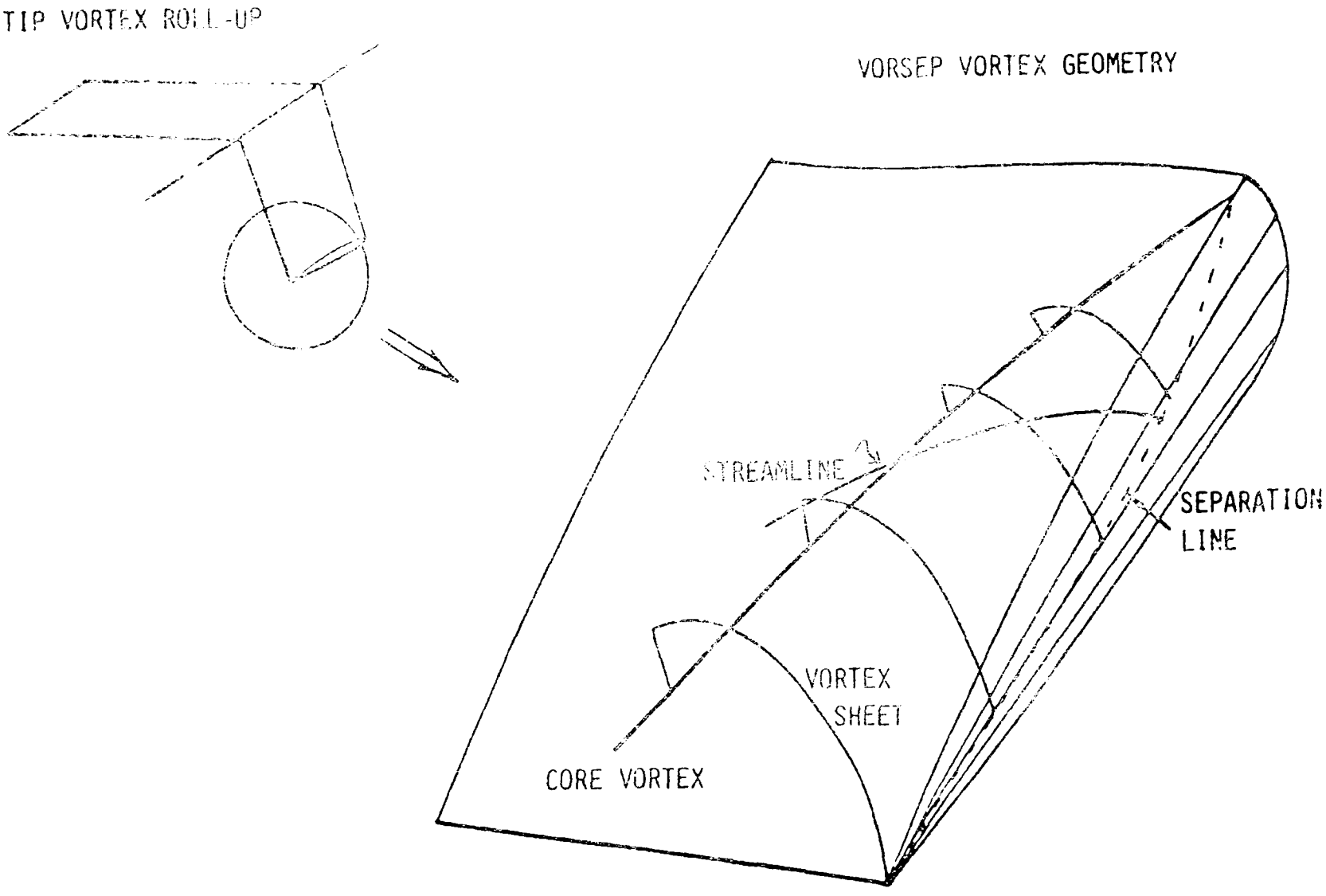

Figure 8. Streamline and Wake Geometry.

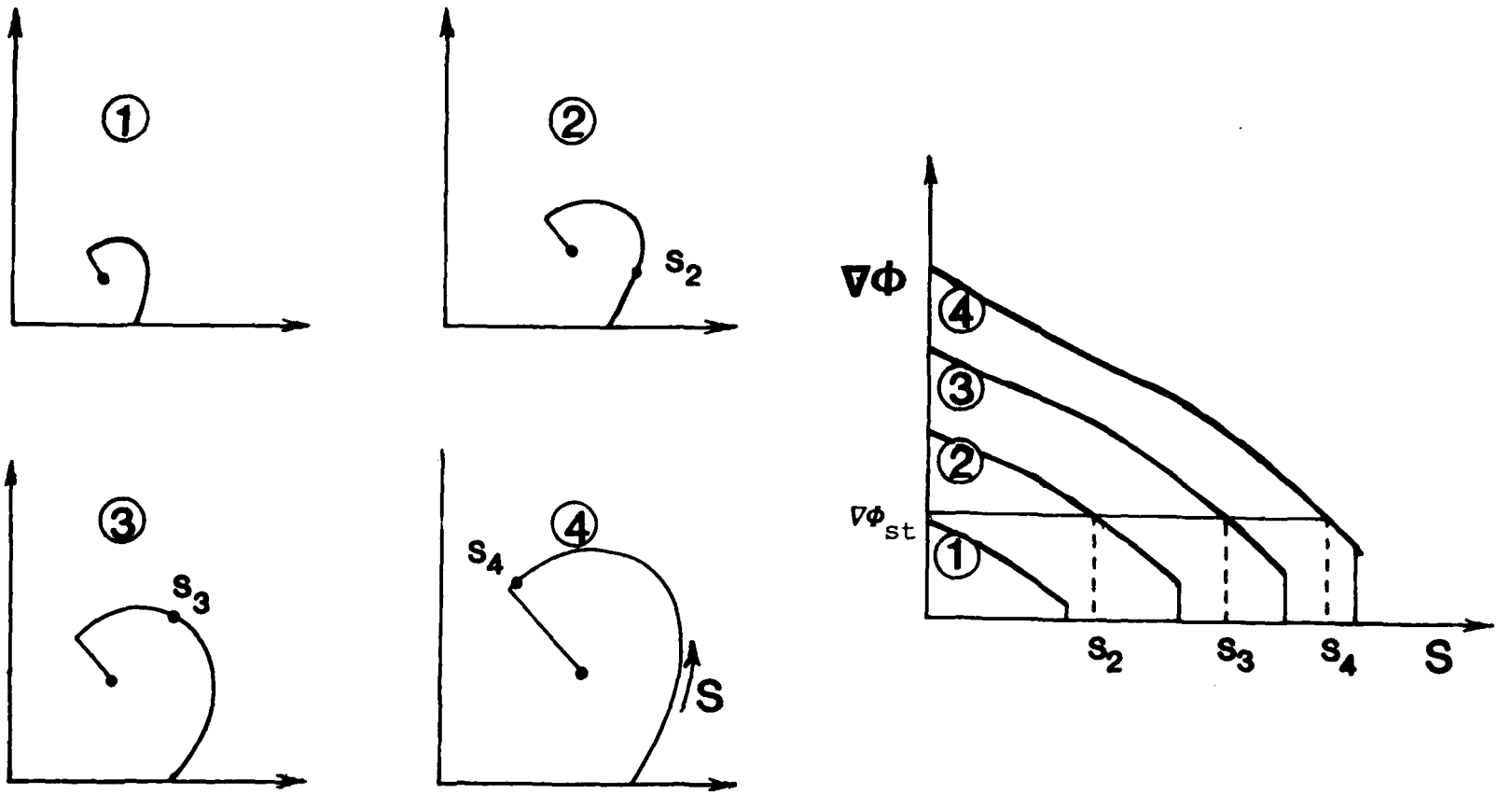

Figure 9. Prediction of Streamline Trajectory from Wake Doublet Distribution.

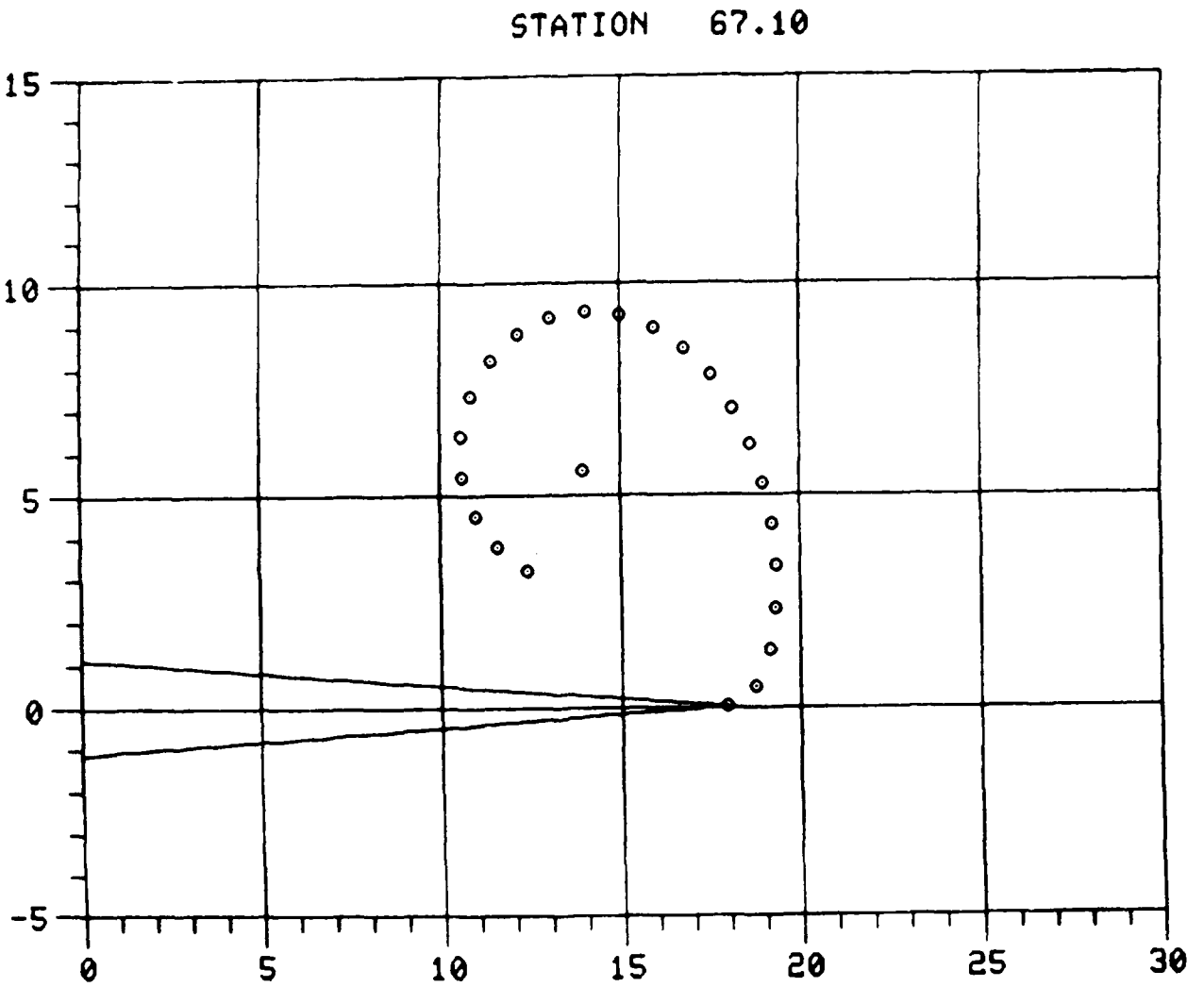

Figure 10. Delta Wing Leading-edge Vortex Shape.

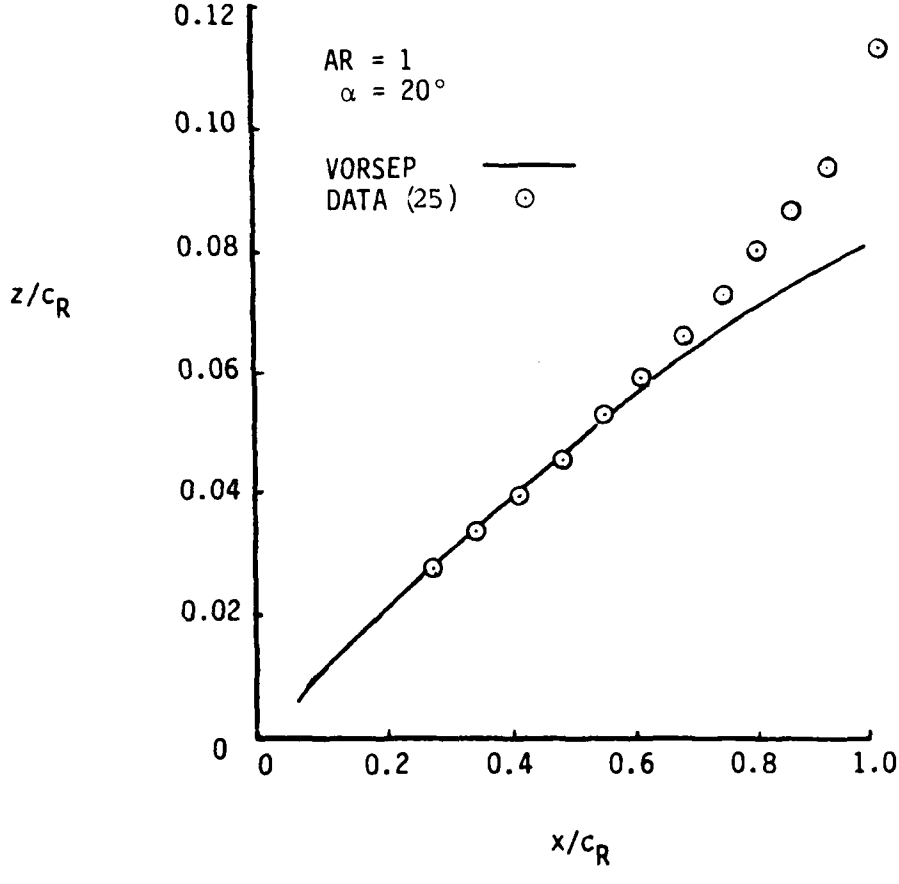

Figure 11 . Predicted and Observed Elevation of Vortex Core over Delta Wing.

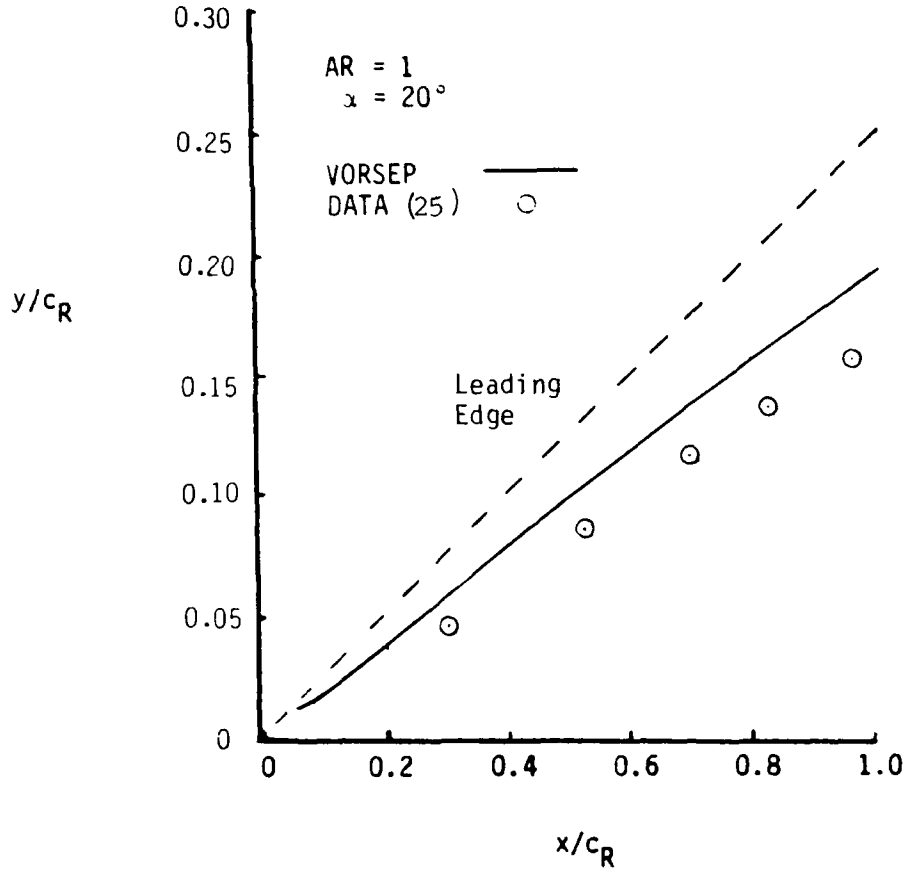

Figure 12. Predicted and Observed Span Position of Vortex Core over Delta Wing.

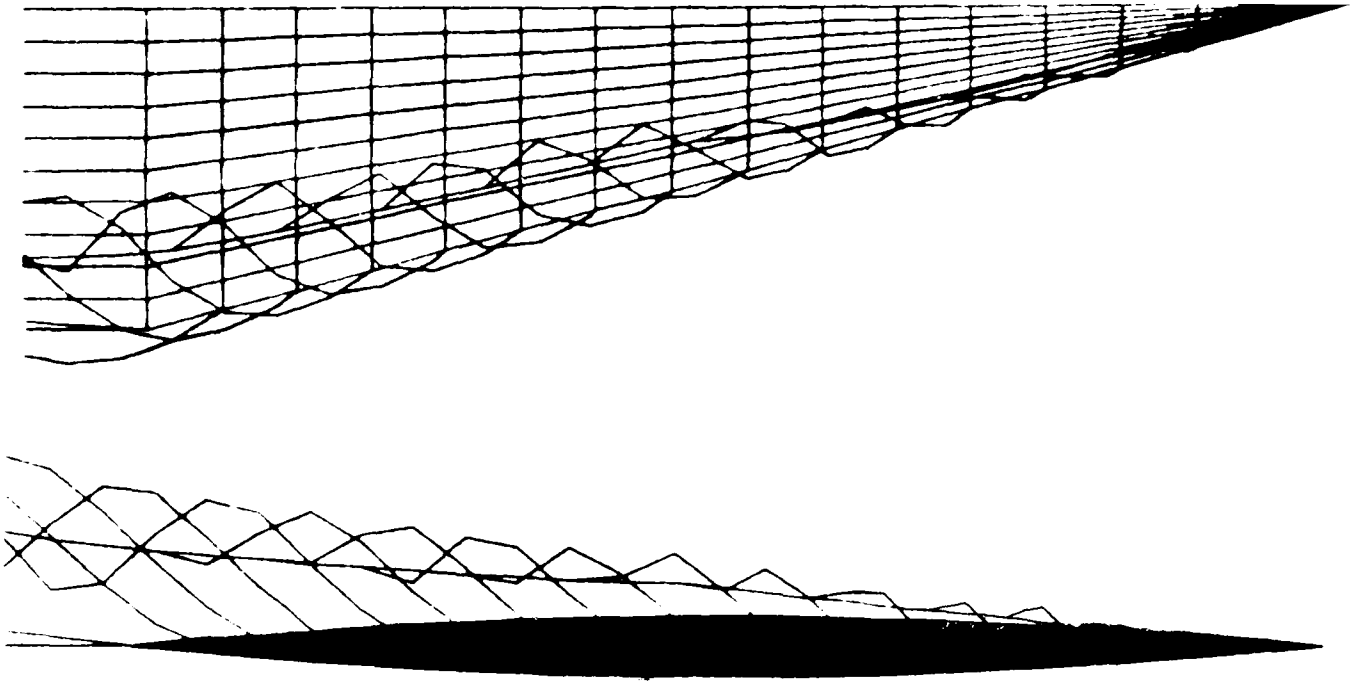

Figure 13. Delta Wing with VORSEP-Generated Leading-Edge Wake.

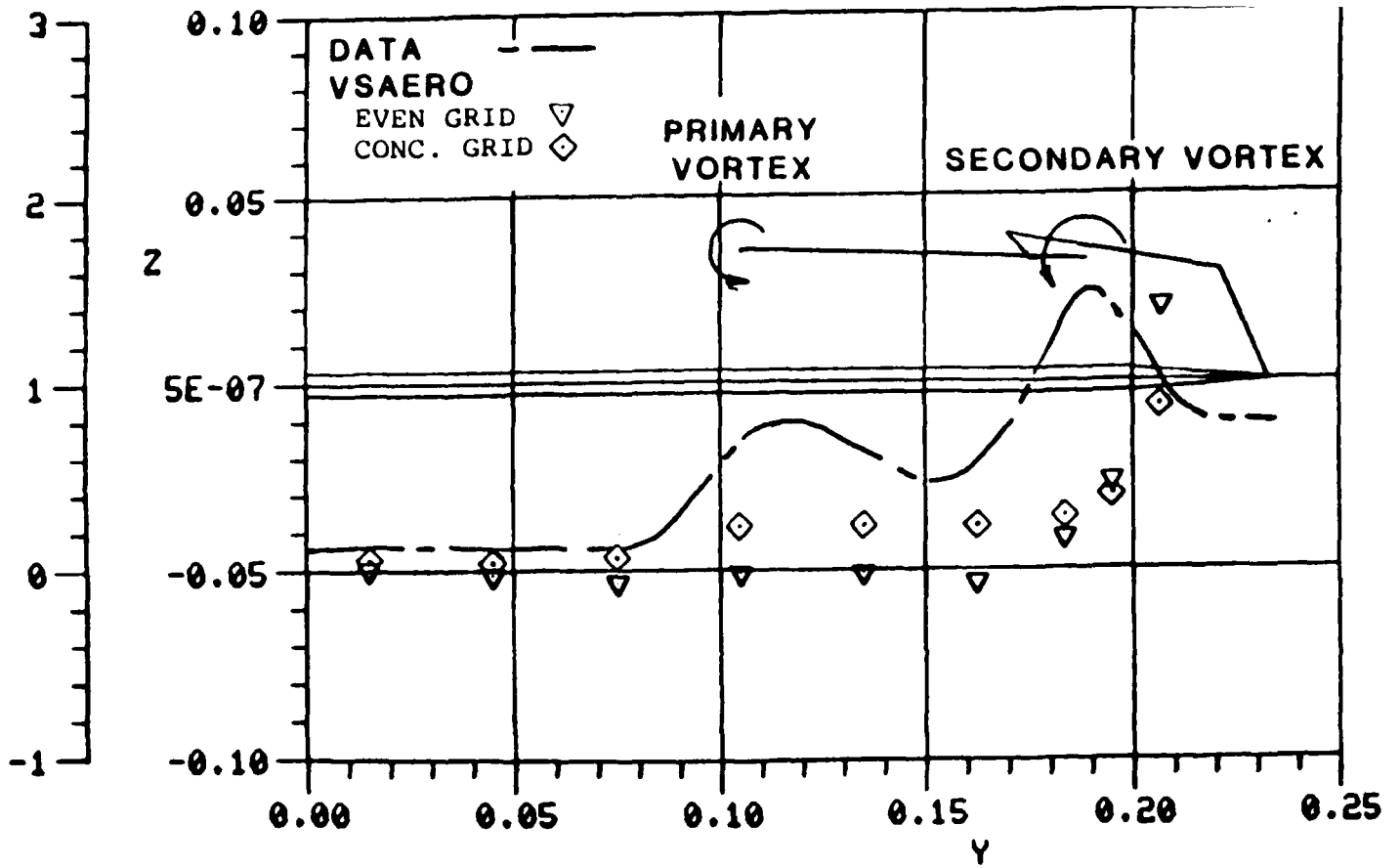

Figure 27. VSAERO Analysis of Hummel Wing at 12°; X = 0.75.

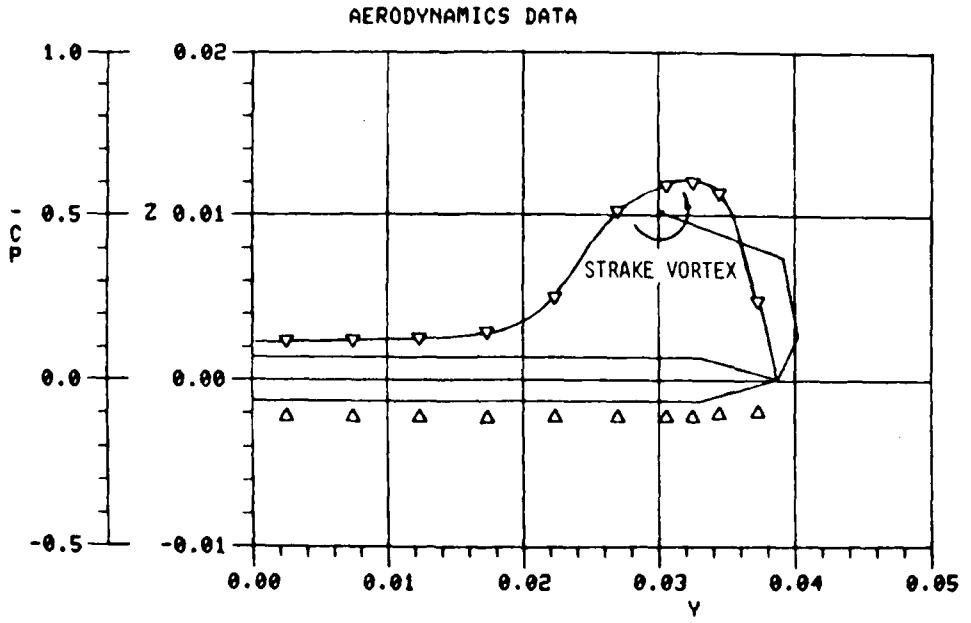

Figure 25. Pressures on Hummel Wing VI at α=10, x=0.22.

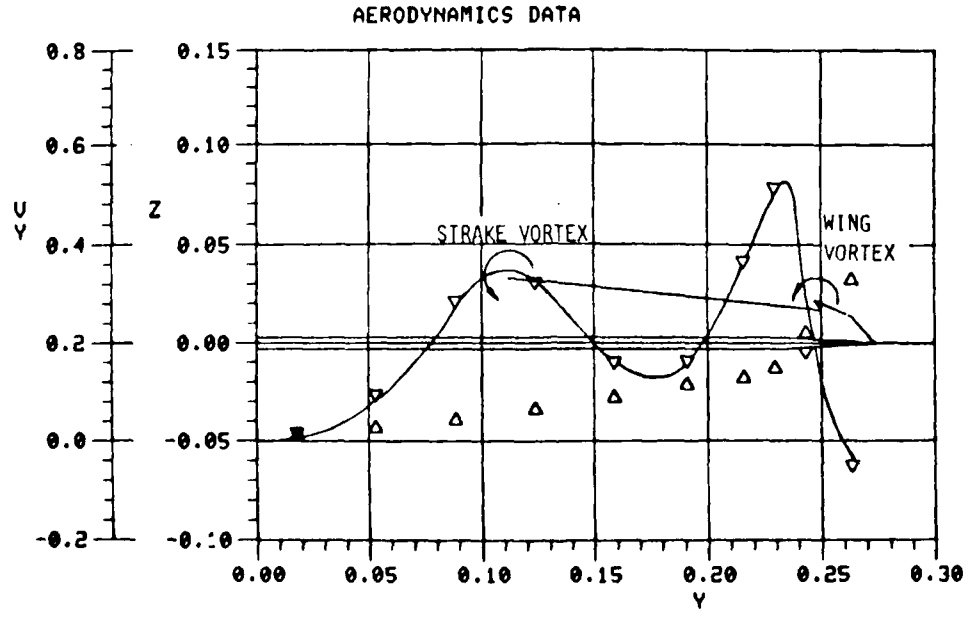

Figure 26. Pressures on Hummel Wing VI at α=10, x=0.82.

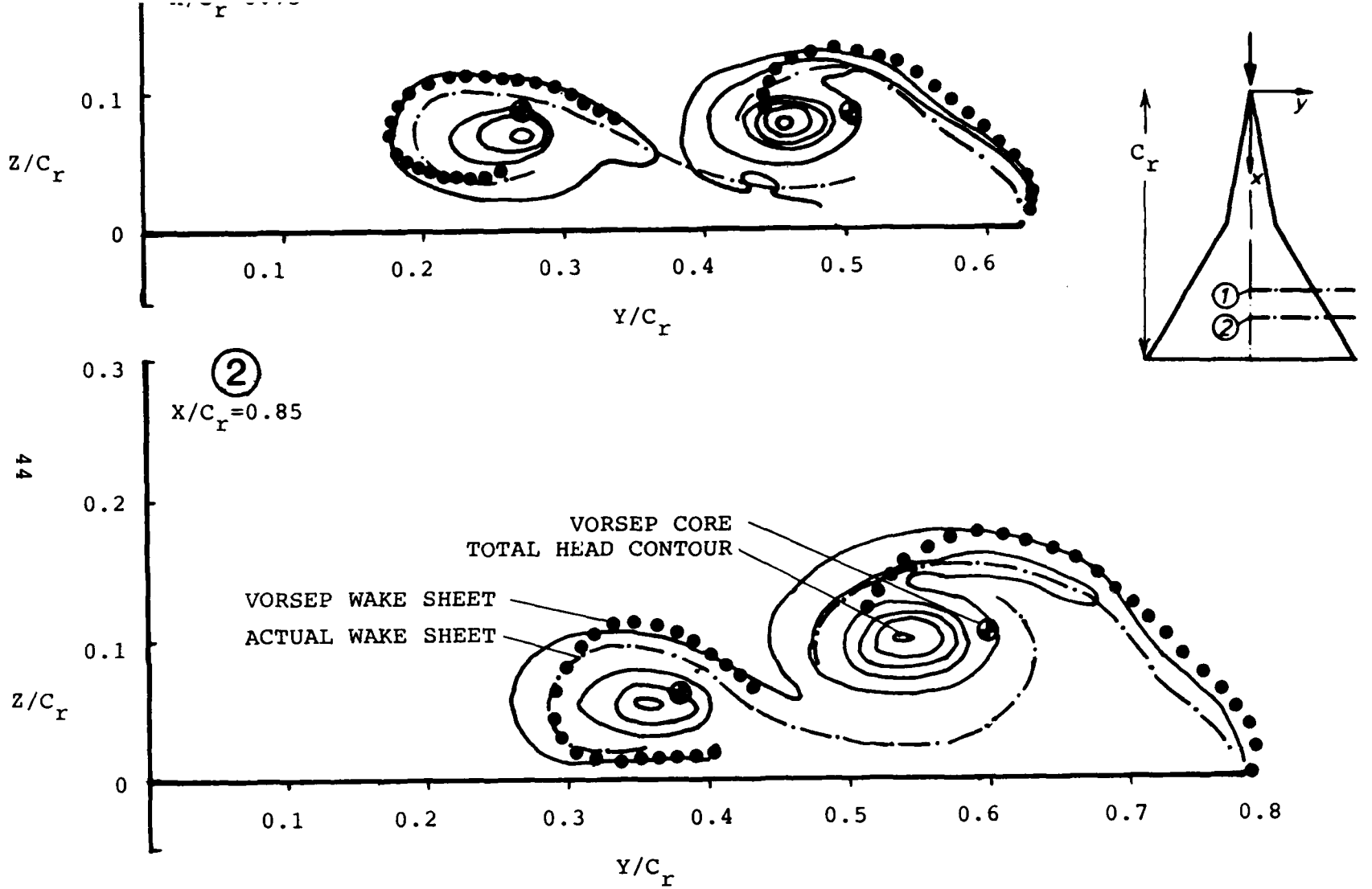

Figure 24. Cross Section of Wake over Double Delta Wing.

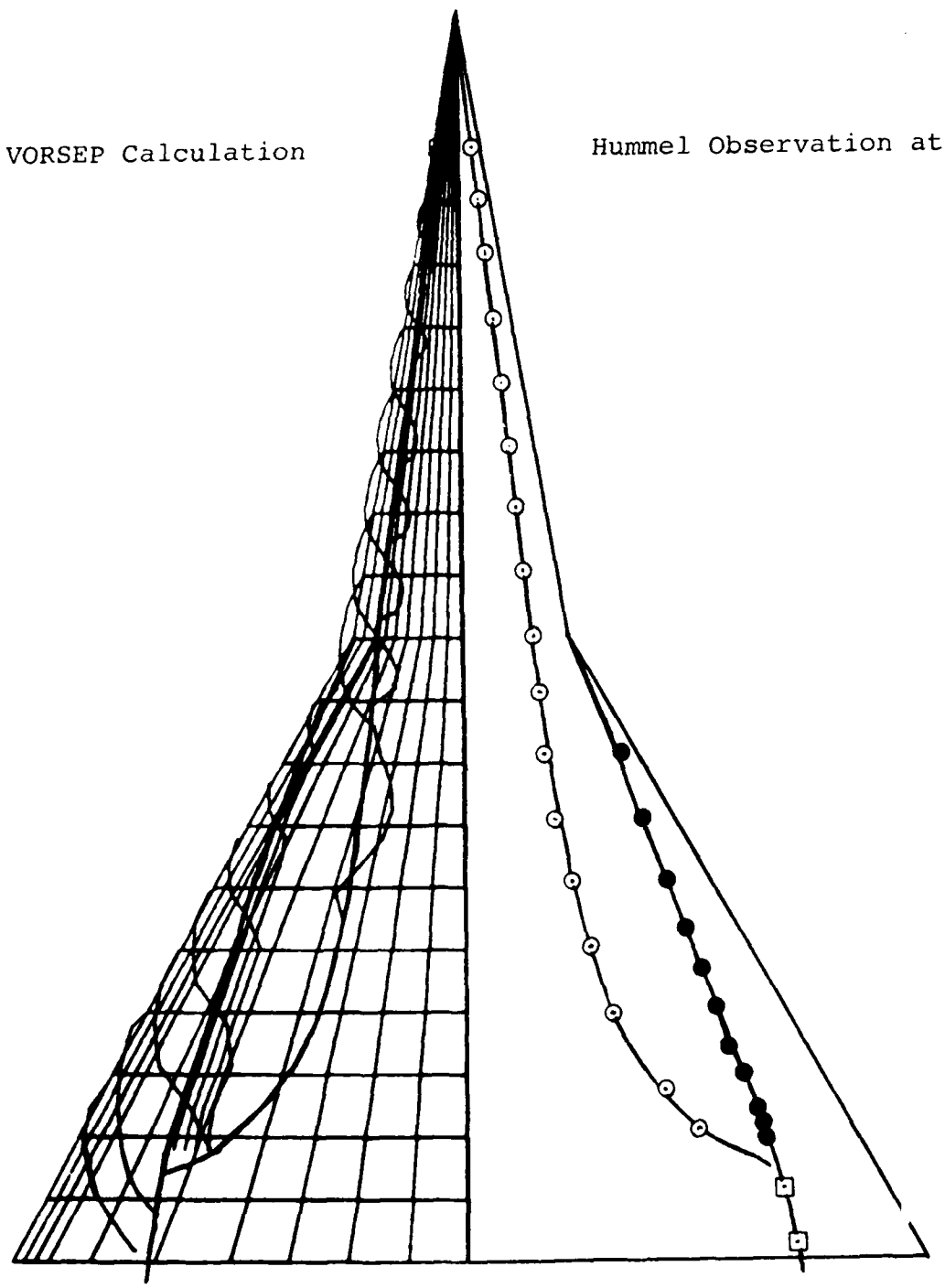

Figure 23. VORSEP Calculation and Observed Wake over Double Delta Wing.

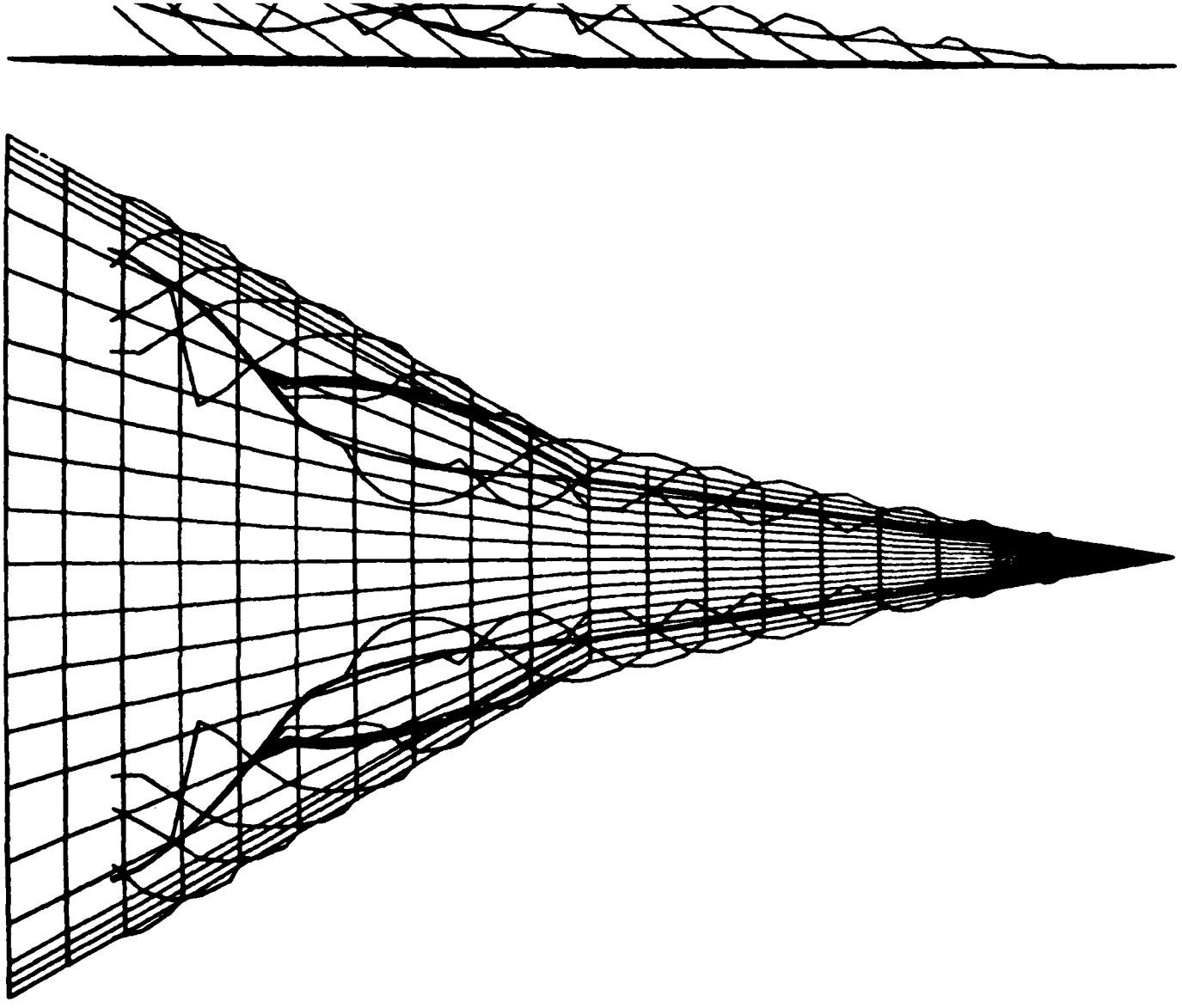

Figure 22. VORSEP-Generated Wake over Hummel Wing VI at 20° .

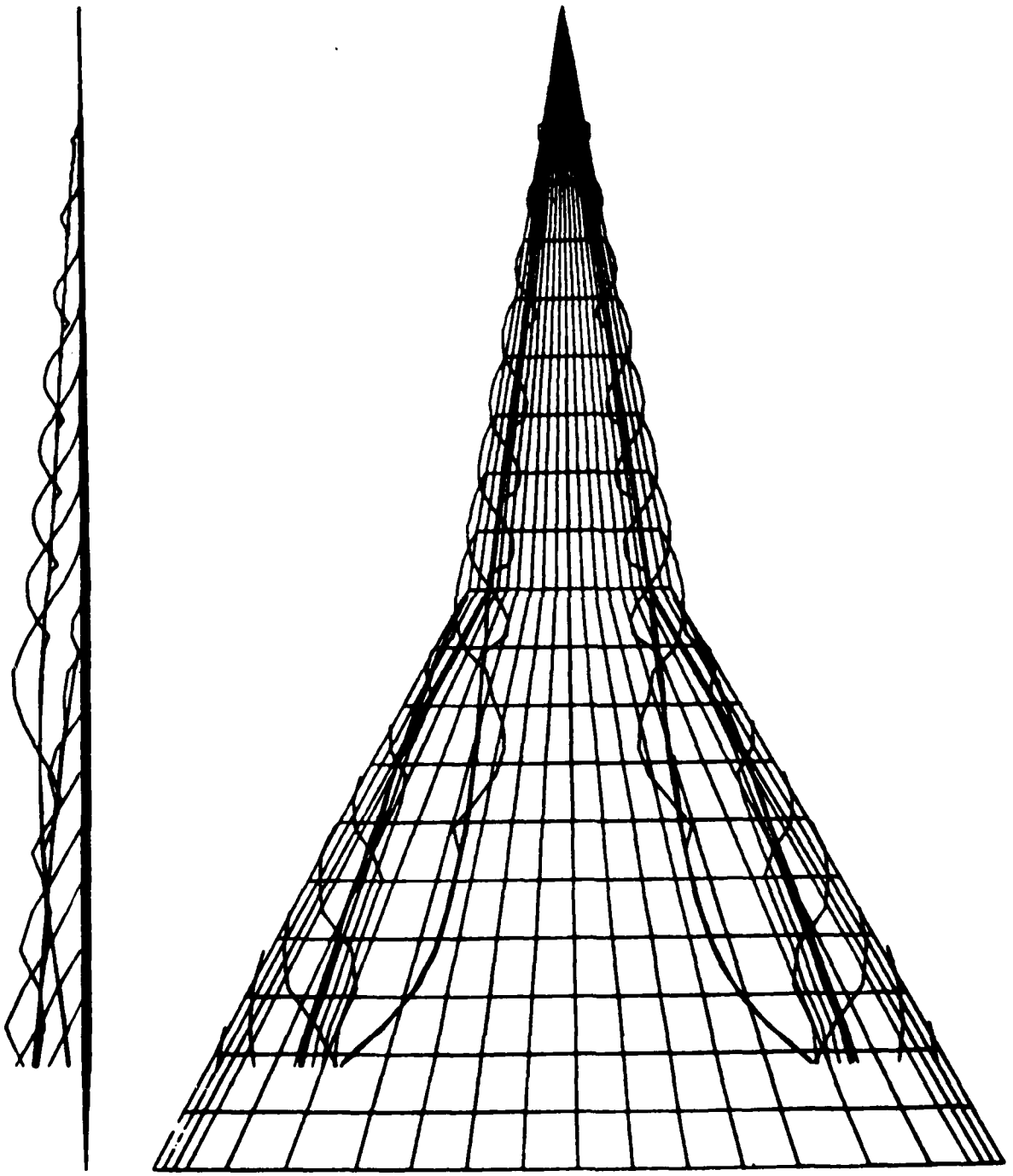

Figure 21. VORSEP-Generated Wake over Hummel Wing VI at 15°.

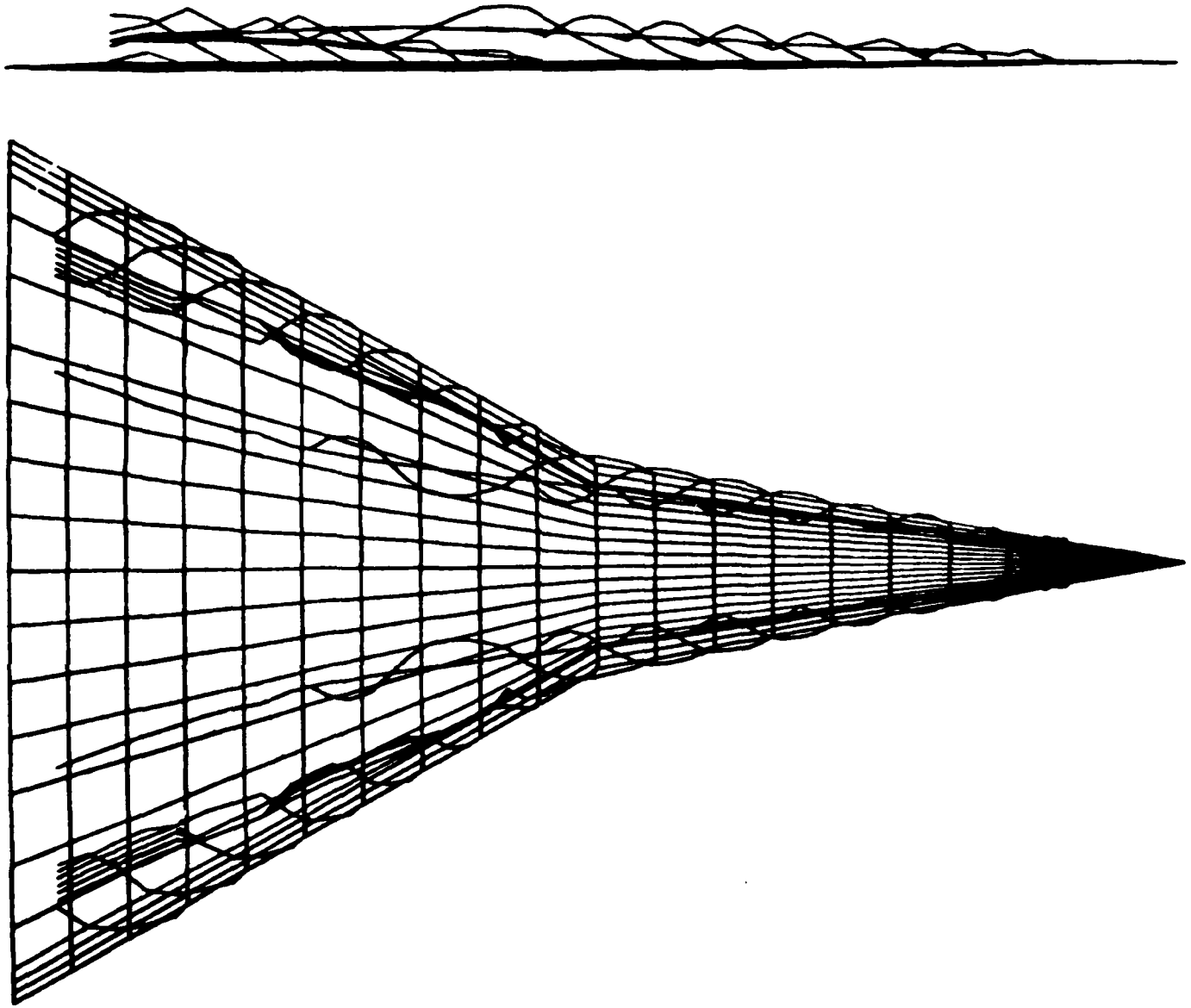

Figure 20. VORSEP-Generated Wake over Hummel Wing at 12°.

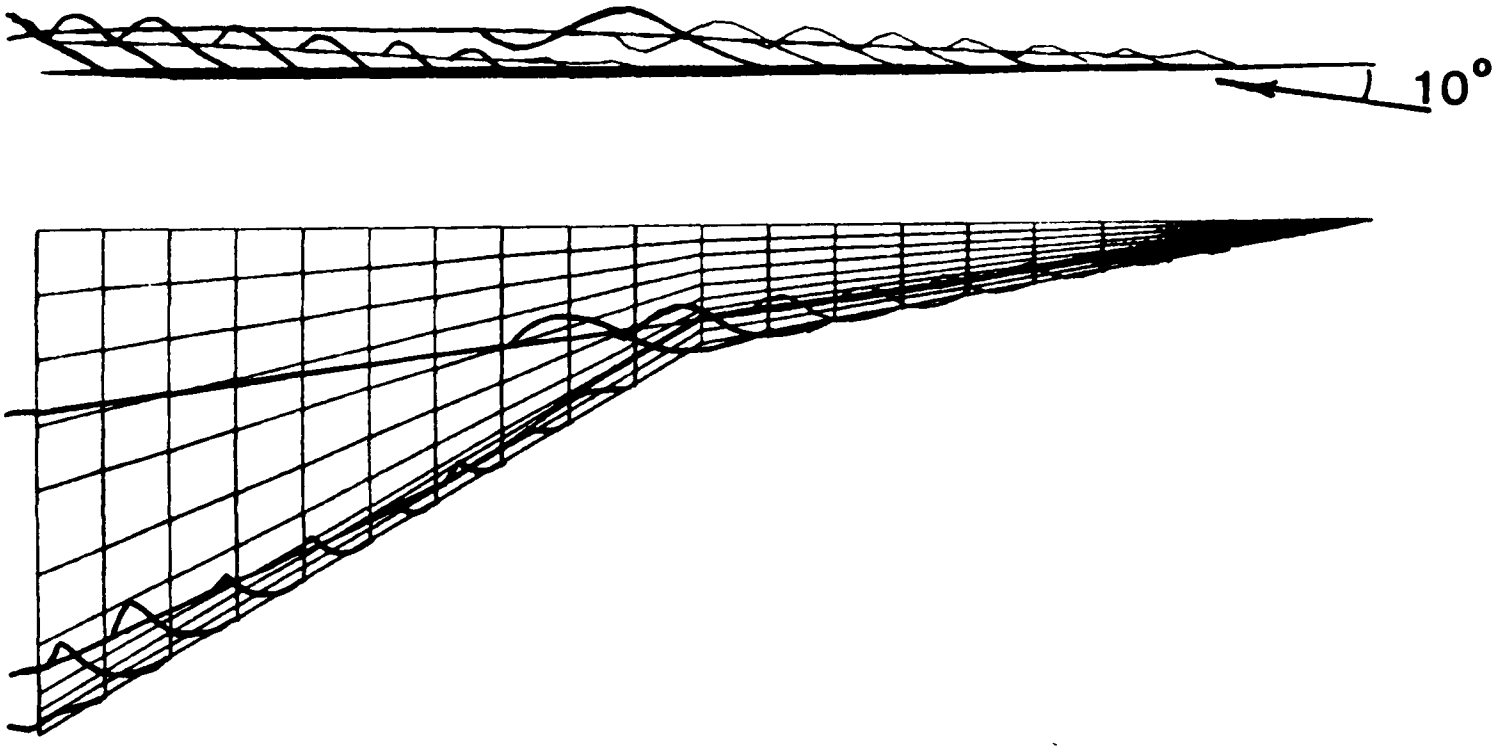

Figure 19. VORSEP-Generated Wake over Hummel Wing VI.

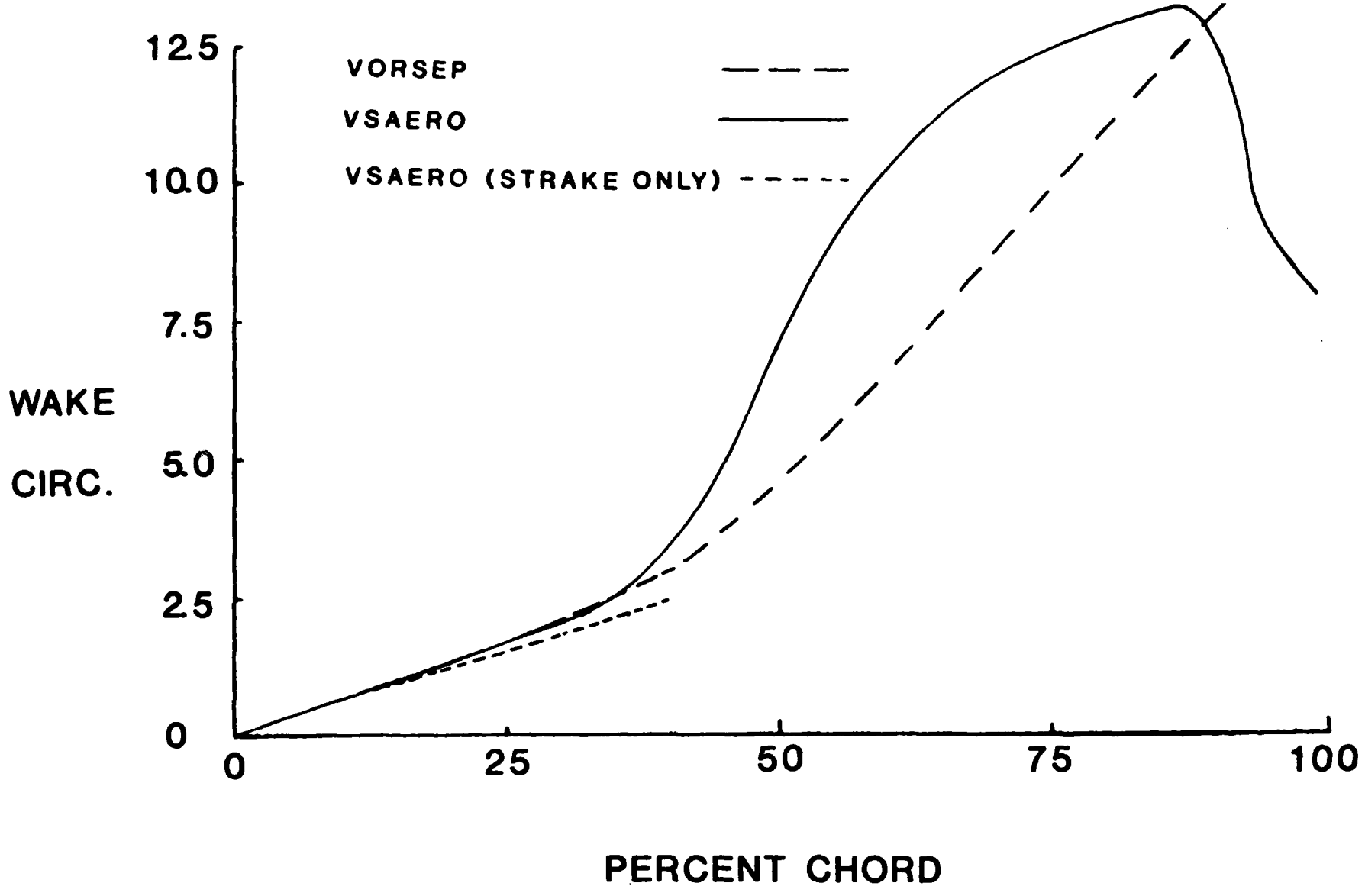

Figure 18. Comparison of VORSEP and VSAERO Vortex Circulation.

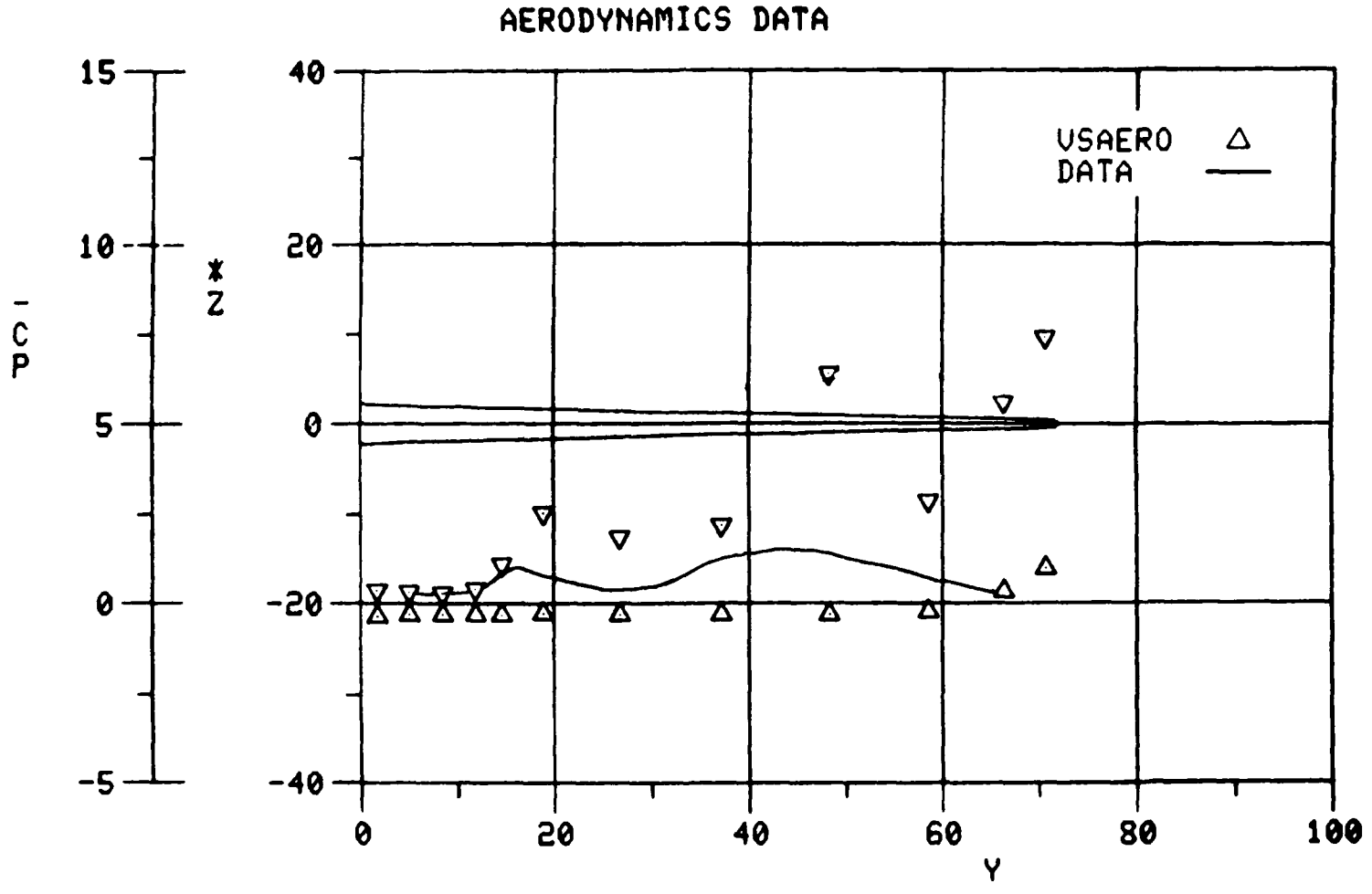

(b) Straked Wing Pressures at 20° Angle of Attack, 50% Local Chord.

Figure 17. Concluded.

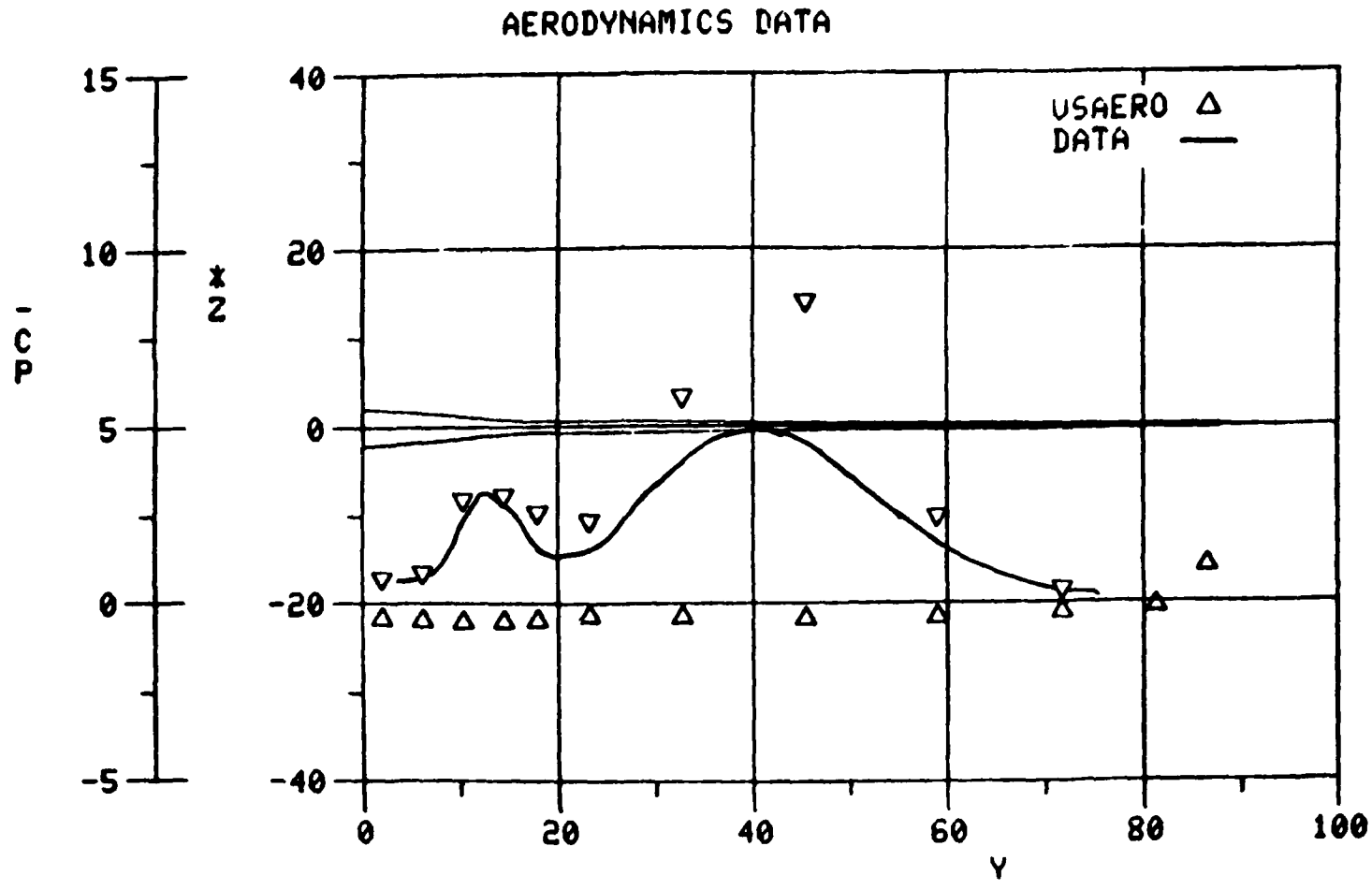

(a) Straked Wing Pressures at 20° Angle of Attack and 10% Local Chord.

Figure 17. Straked Wing with VORSEP-Generated Wake.

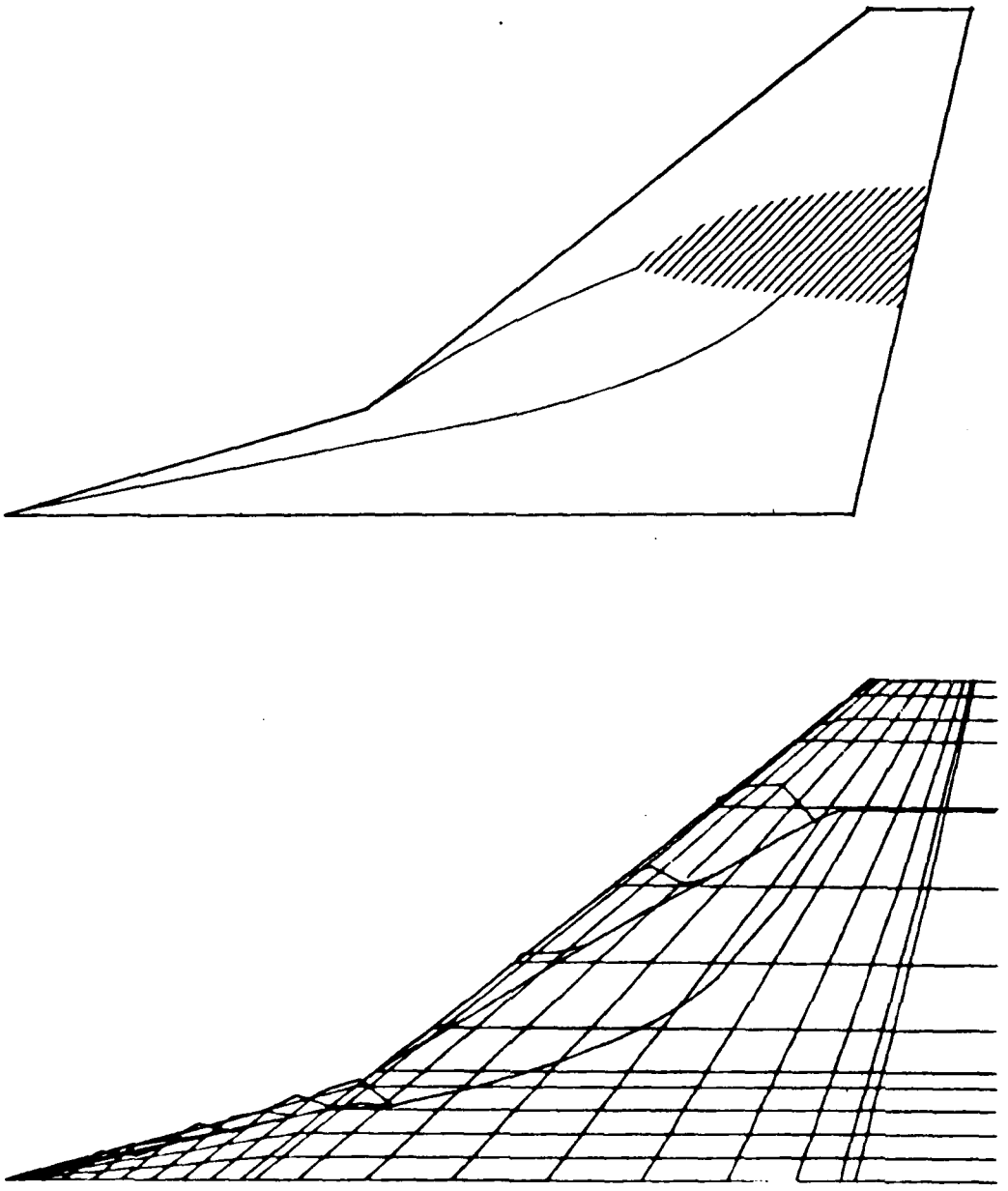

Figure 16. VORSEP Calculation and Observed Wake on Swept Wing with Strake.

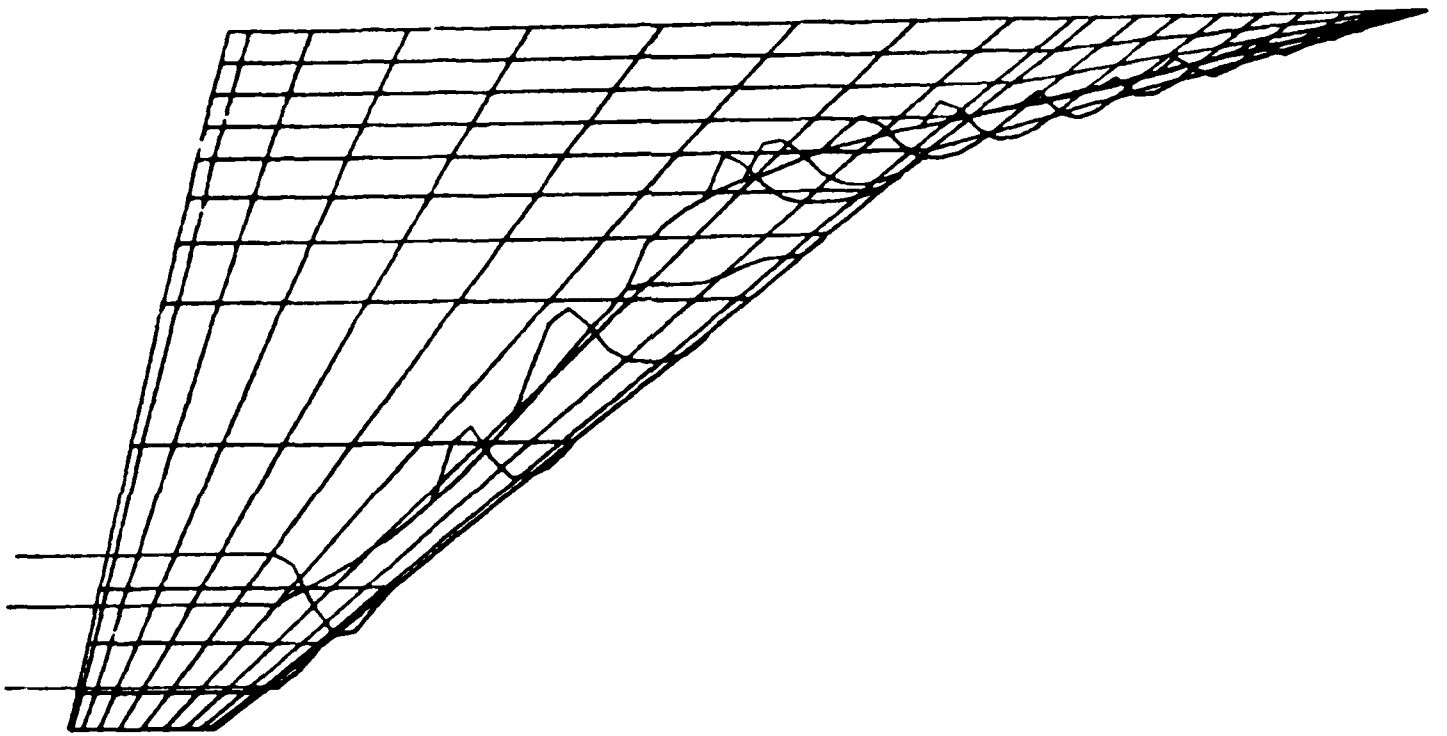

Figure 15. Single-Wake Model of Leading-Edge Separation over Straked Wing.

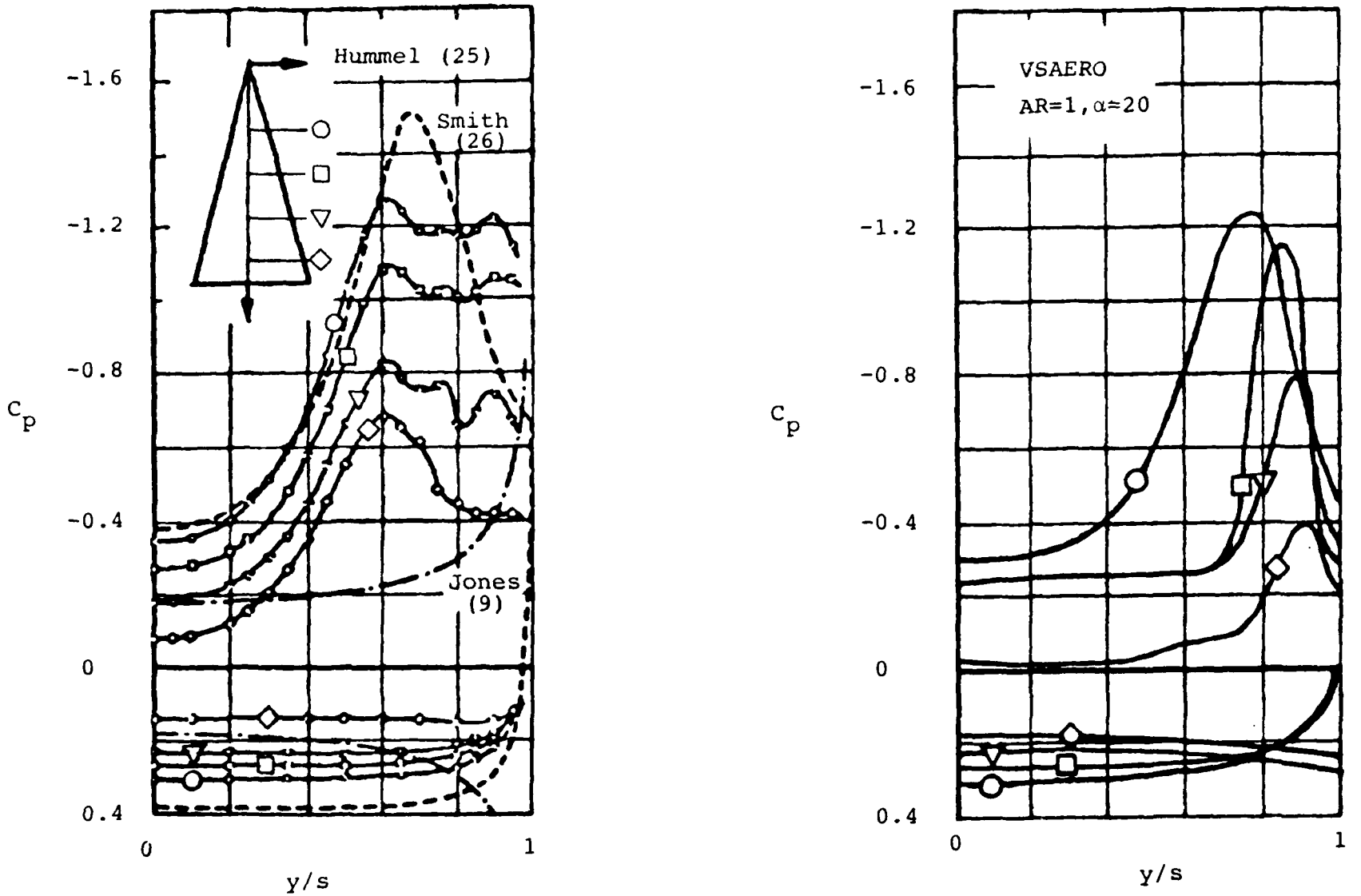

Figure 14. Comparison of VSAERO Pressure Distribution on Delta Wing with Experiment.

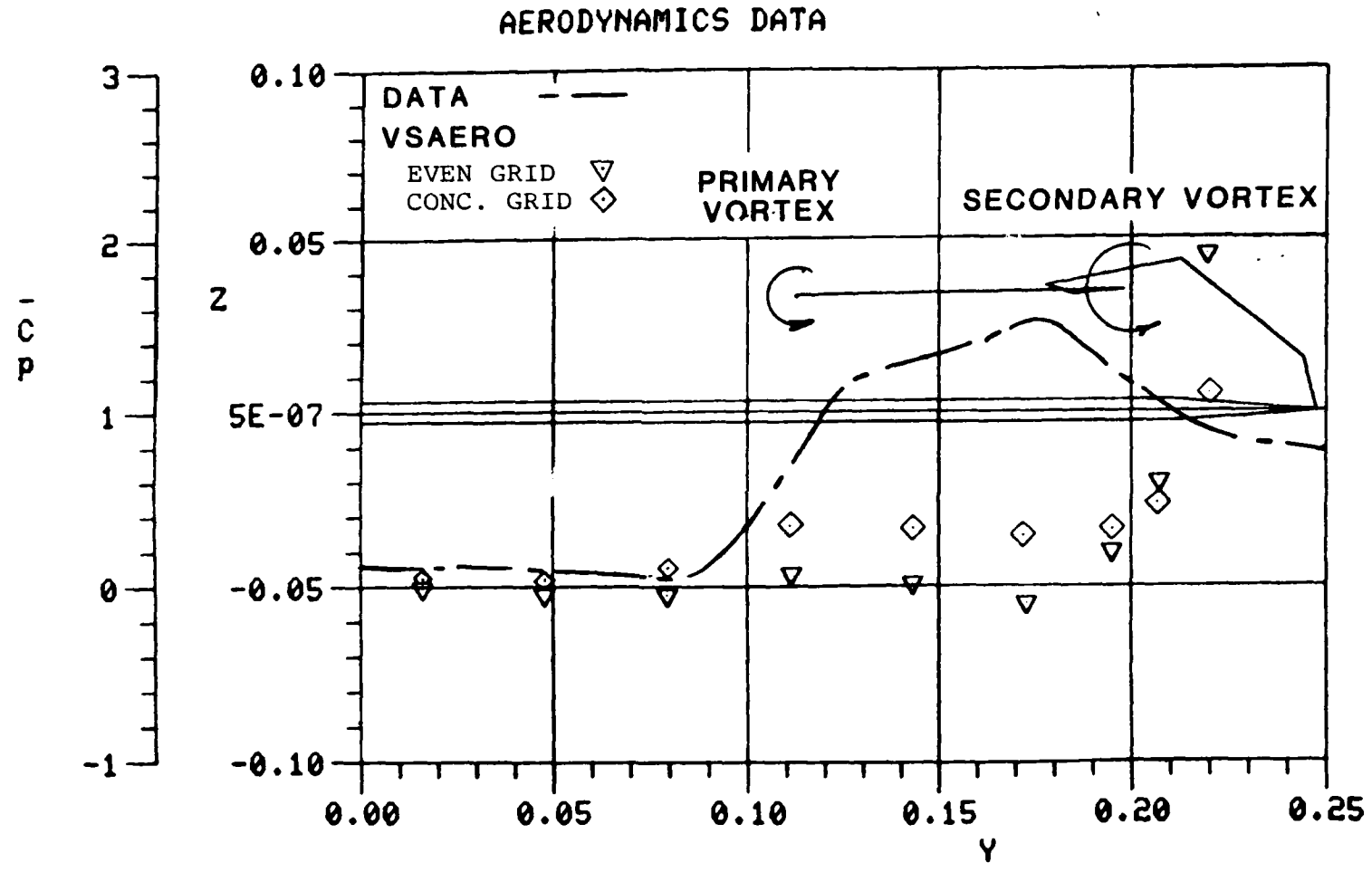

Figure 28. VSAERO Analysis of Hummel Wing at 15°, X = 0.77.

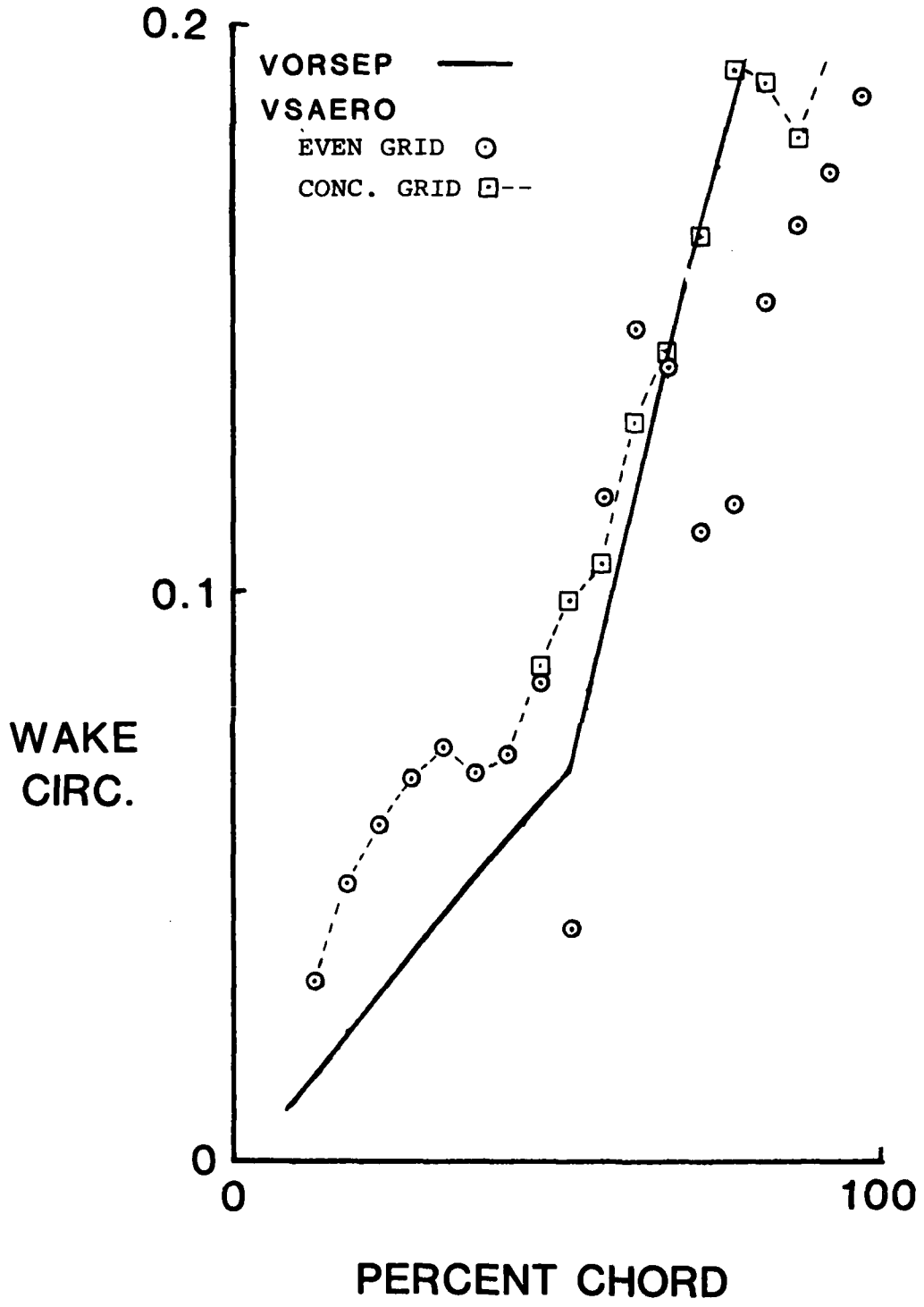

Figure 29. Comparison of VORSEP and VSAERO Circulation for Double-Delta Wing.

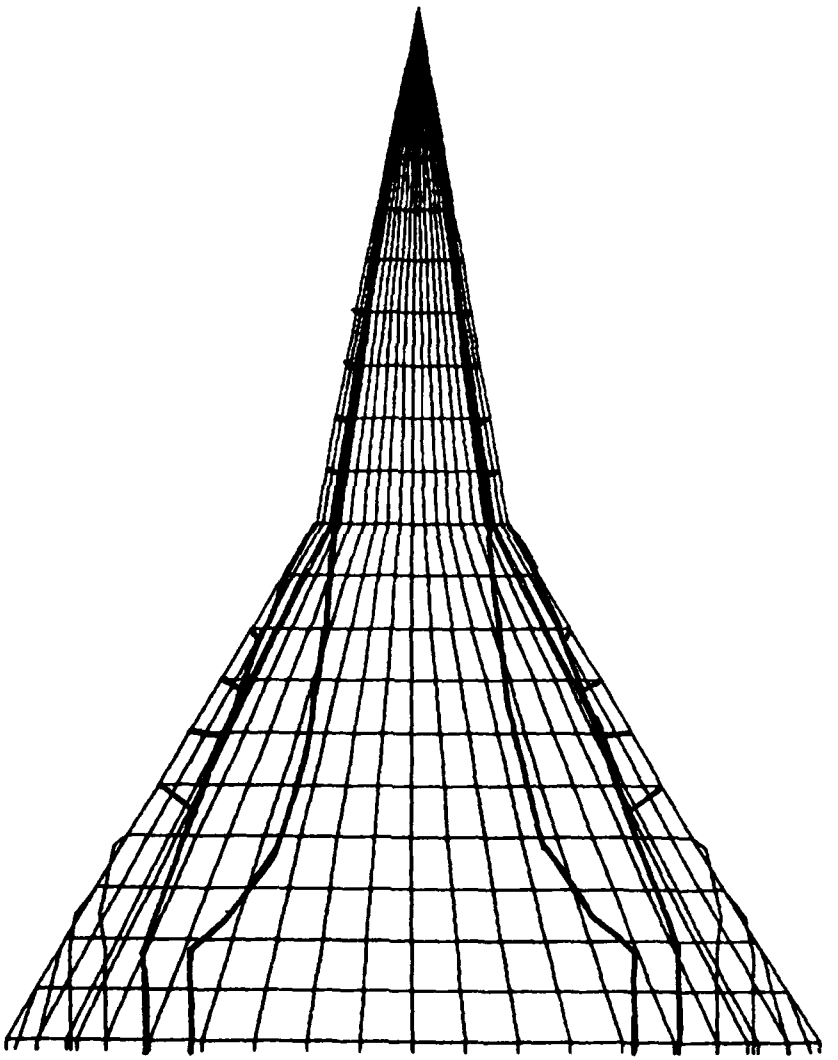

Figure 30. Hummel Wing VI with Simplified Wake Model.

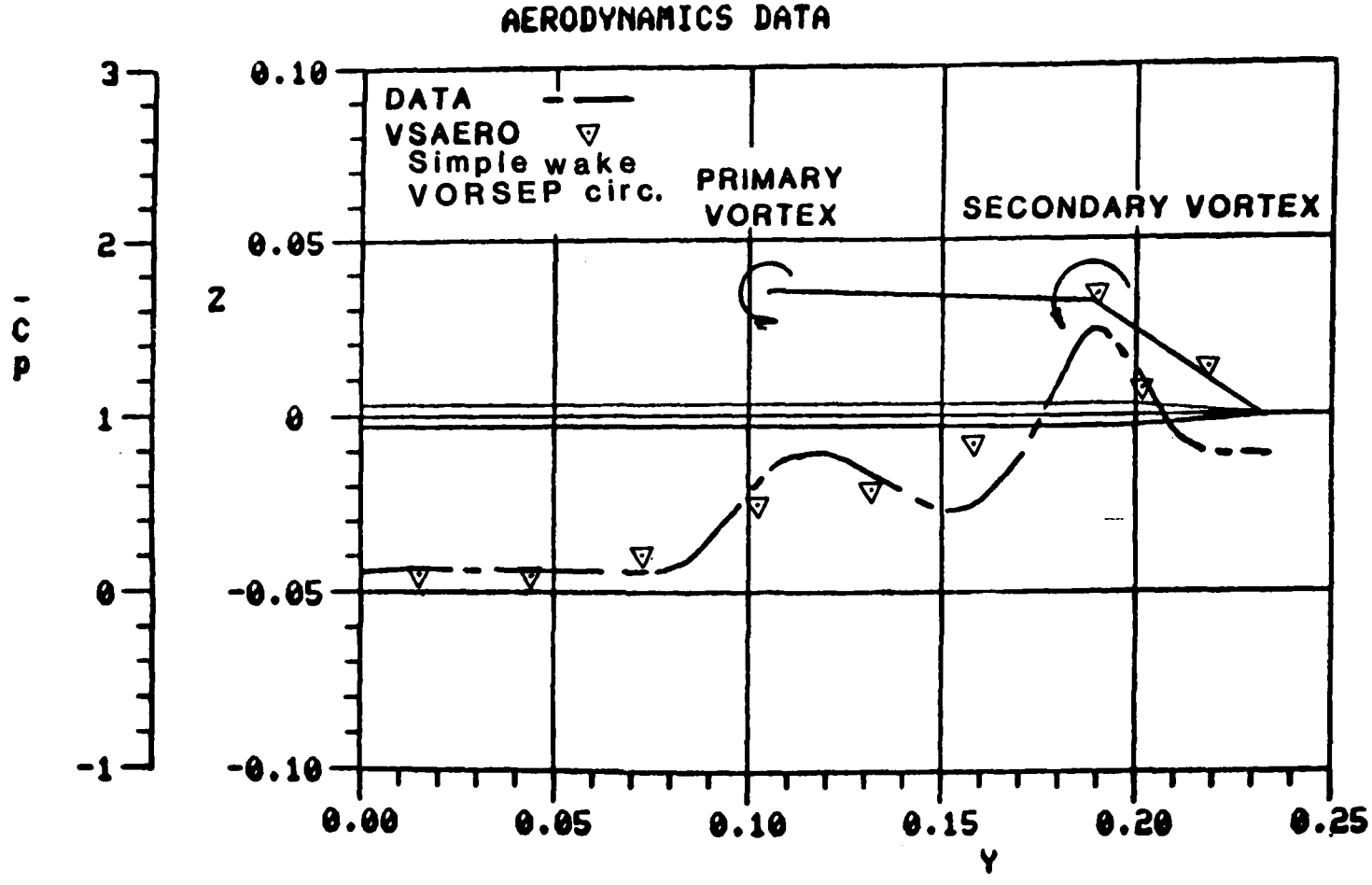

Figure 31. VSAERO Analysis of Hummel Wing at 12°; X = 0.75.

APPENDIX

VORSEP USER'S GUIDE

Revision 1.0

VORSEP USER'S GUIDE

VORSEP is a program designed to calculate the geometry of wakes produced by separation from swept leading edges such as the leading-edge vortices over delta wings. VORSEP was developed on a Prime 550 minicomputer. However, only minimal changes to the FORTRAN IV source code should be necessary for it to run on any other system. The system should have the Tektronix TCS and AGII graphics libraries, the same as those used by OMNIPLOT, the graphics program for VSAERO. Indeed, VORSEP is designed to interact with VSAERO and OMNIPLOT, so it is recommended that the entire suite of codes be on the same system.

VORSEP requires as input a basic input file (logical file 5) and a body geometry file (logical file 11). The body geometry file can be generated with VSAERO. This is logical file 7, the plot file, in VSAERO. For faster VORSEP execution any patches ahead of or behind VORSEP calculations should be left out. Also, the plot file need not contain any wakes, (MSTOP=2 in VSAERO data). It is better now to determine the body paneling under the separated wake because the starting points of the wake streamlines are needed by VORSEP and the greater detail will give better results from VORSEP.

The file structure for VORSEP is listed in Table 1. After creating a basic input file according to the input guide VORSEP can be run with the following in mind:

a) A typical delta wing with leading-edge separation requires approximately 150 time steps from 10% root chord to trailing edge. Average CPU time per time step is 30 seconds on a Prime 550.

b) Tracking streamlines is inexpensive so start streamlines everywhere panel corners are or might be later on.

c) Each calculation plane can be plotted with NEWPLT. The plot information is written by VORSEP to logical file 12. To execute NEWPLT, simply open the cross-flow geometry file from VORSEP as logical file 12 and execute the program. NEWPLT will ask for the horizontal and vertical scales as well as the number of decimal digits in the station format, see Figure A-1. NEWPLT will plot every station automatically requiring the user to 'return' after each plot.

d) If a restart is made then the wake output file (logical file 13) must not be overwritten by the restart. Accumulate this output in a separate file, each new output file being added to the bottom.

Once VORSEP execution is completed, the wake streamline geometry can be generated with WAKGEN. This program reads the cross-flow geometry produced by VORSEP and outputs the wake streamline geometry, which with minor editing is the wake geometric description used in VSAERO. WAKGEN will also combine the wake information with the body geometry file to produce a graphic streamline data file. This file has the same format as an OMNIPLOT plot file and can be plotted directly to illustrate the wake streamlines before any VSAERO modification, for example, Figure 2. The file structure for WAKGEN is listed in Table 2.

Table 1. VORSEP File Structure

Logical File	Description
5	Basic VORSEP input
6	Printer output
7-10	Disk scratch files
11	Body geometry input
12	Cross-flow geometry graphic output
13	Wake streamline output

Table 2. WAKGEN File Structure

Logical File	Description
6	Wake geometry output for VSAERO
11	Body geometry input
13	Wake geometry from VORSEP
14	Body & wake graphics output

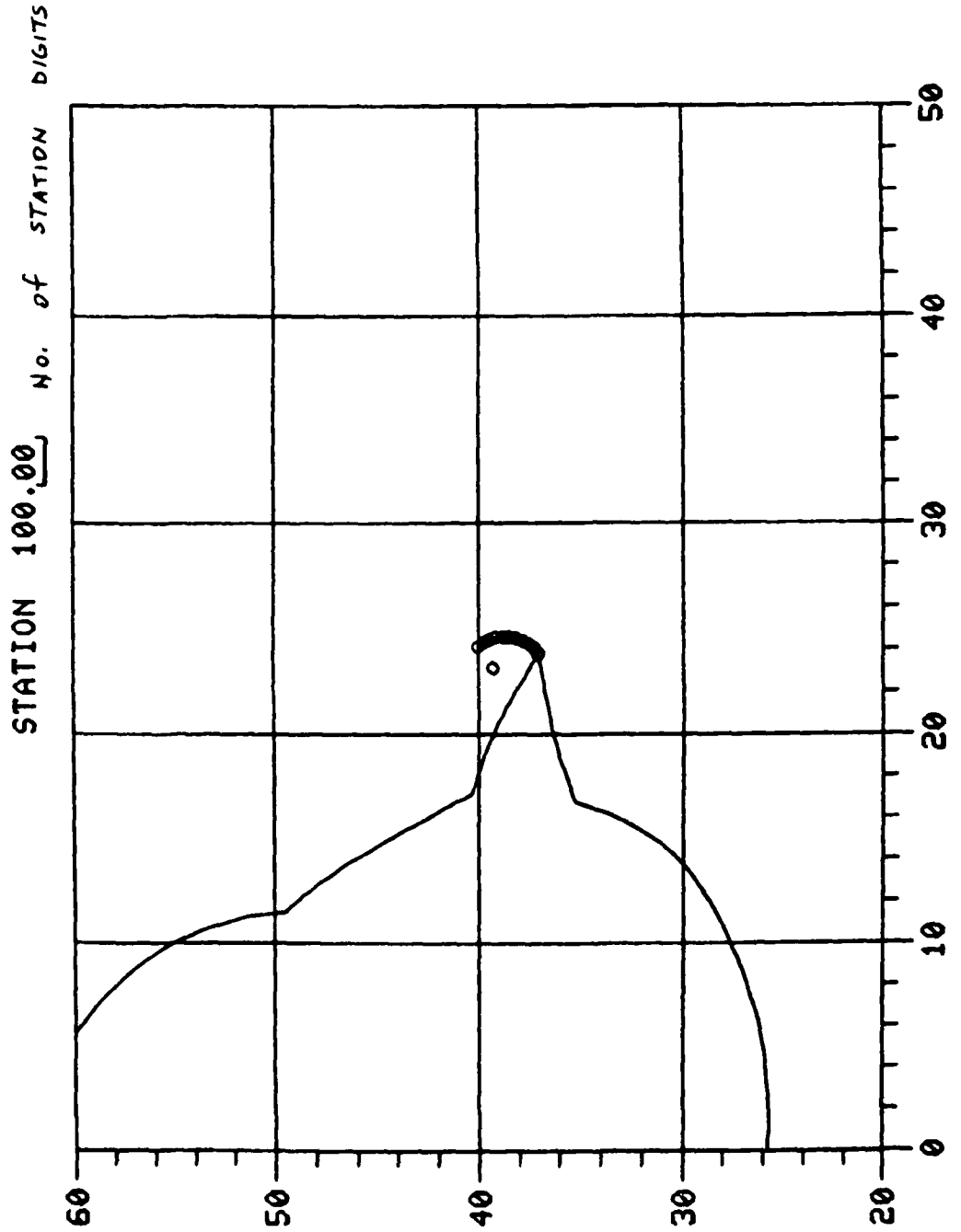

Figure A-1. Sample Output from NEWPLT.

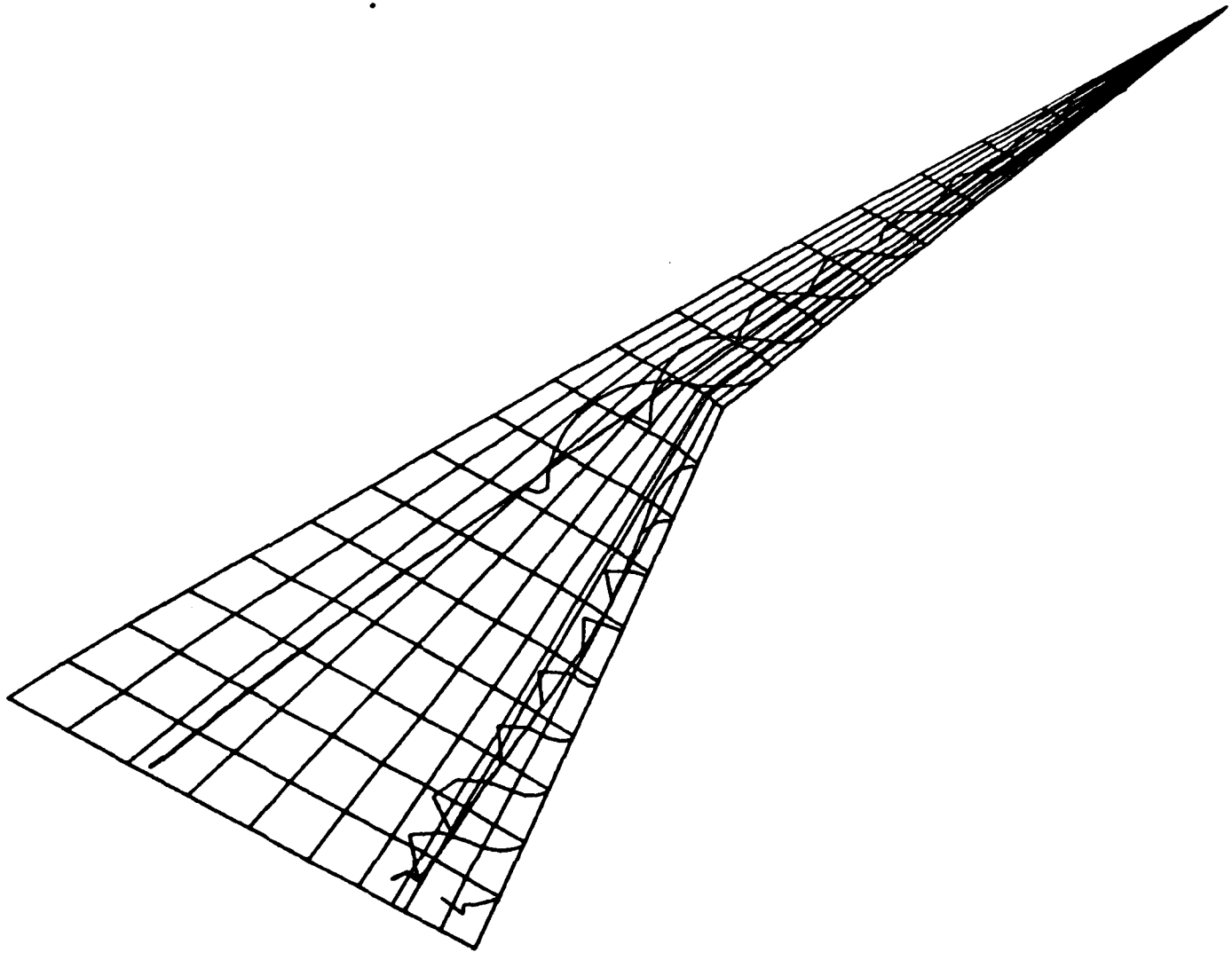

Figure A-2. Wake Geometry Output from WAKGEN Plotted with OMNIPLOT.

VORSEP INPUT DESCRIPTION

Values given in parentheses are suggested values unless identified otherwise.

CARD 1: Title

Column	Variable	Description	Format
1-80	TEXT	Title information	20A4

CARD 2: Print Control

Column	Variable	Value	Description	Format
1-5	IPRI	1	Input data printed	3I5
		0	Off	
6-10	IPRLEV	0	Wake geometry and potential solution printed	
		1	Panel geometry and surface velocities also printed	
		2	Pressure distribution printed	
11-15	IPRINT	≥0	Time steps between print-outs	

CARD 3: Symmetry Card

Column	Variable	Value	Description	Format
1-5	ISYM	0	No symmetry	I5
		1	Lateral symmetry	

CARD 4: Operating Conditions

Column	Variable	Value	Description	Format
1-10	ALPHI		Free stream angle of attack (deg) relative to y-axis	3F10.0
11-20	ALDEG		Sideslip angle (deg)	
21-20	NFR	(3.5)	Near-field radius for panel influence	

CARD 5: Section Definition

Column	Variable	Value	Description	Format
1-10	STX	0.0	Location of section local coordinate system origin in the general coordinate system.	4F10.0, 2I5
11-20	STZ	0.0		
21-30	SCALE	1.0	Scaling factor to be applied in the local coordinate system	
31-40	THETA	0.0	Orientation of local coordinate system relative to the general system's x-axis	
41-45	INPUT	0	Standard form of geometry input. Requires CARDS 12, 13 and 14	
46-50	IDENT	0	Thick section	

CARD 6: Time-Step Definition

Column	Variable	Value	Description	Format
1-5	NTIMEX	(>0)	Number of time steps between wake grid planes	2I5
6-10	NWGP		Number of wake grid planes (CARD 7)	

CARD 7: Wake Grid Plane Definition

Column	Variable	Description	Format
1-10	WGPX(1)	First wake grid plane station	8F10.0
11-20	WGPX(2)	Second station	

.
.
.

D 8: Separation Line Specification

umn	Variable	Value	Description	Format
10 20 20	XSEP YSEP ZSEP		Coordinates describing separation line geometry	3F10.0, I5
35	NODE	(0)	First or intermediate point on line	
		(3)	Last point on this separation line (i.e., next CARD 8 begins another separation line)	
		(5)	Last CARD 8	

es: If NODE ≠ 0, XSEP, YSEP and ZSEP must still be physical values.

Repeat CARD 8 as many times as required to define all the separation lines.

3D 9: Merge Angles

lumn	Variable	Description	Format
-10	THMERG(1) . . .	Maximum roll-up angle (deg) for primary vortex core (specify as many merge angles as separation lines on CARD 8)	8F10.0
	T2MERG	Maximum roll-up angle (deg) for secondary vortex core	
	XSEP2	Station along first separation line at which secondary core originates	

te: Only the first wake specified by the first separation line on CARD 8 can have a secondary vortex core.

If XSEP2 is 0.0 or left blank, it is assumed there is no secondary core for wake 1.

CARD 10: Restart Card

Column	Variable	Value	Description	Format
1-5	LSEP(1)	(0)	Wake has not started	4I5
		(1)	Wake has started (requires CARDS 11A and B)	
	.			
	.			
	.			
16-20	LSEP(4)		"	

CARD 11A: Wake Geometry (Only present for a restart)

Column	Variable	Description	Format
1-5	NPAN	Number of wake panels	2I5
6-10	NPAN2	Number of secondary wake panels for multi-core wake	

CARD 11B: Wake Geometry (Only present for a restart)

Column	Variable	Description	Format
12-21	WX	Vortex y-position	11X, 2F10, 10X, 2F10
22-31	WZ	Vortex-z position	
42-51	WD	Wake corner doublet strength	
52-61	WDUB	Wake panel doublet strength	

Note: CARD 11B is repeated NPAN+1 times for each wake that has already started. The format is exactly that of the output file from VORSEP.

CARDS 11A and B are repeated for each wake which has already started.

12: VSAERO Geometry Description

mn	Variable	Description	Format
	NPATCH	Number of patches in VSAERO geometry file	I5

(S) 13: Patch Definition

mn	Variable	Description	Format
	IPAN(1)	First panel on Patch 1	16I5
0	LPAN(1)	Last panel on Patch 1	
5 0		Same as above for Patch 2	
5 0		Same as above for Patch 8	

: Repeat CARD 13 as necessary if more than 8 patches.

14: Automatic Paneling Parameters

mn	Variable	Description	Format
.0	ANGTOL (0.25)	Tolerance to define discontinuous geometry between two three-dimensional panels. $\cos^{-2}\theta$ where θ is acute angle between three-dimensional panel and exterior of previous panel	3F10.0, I5
.5	DENS (3.0)	Factor to multiply number of three-dimensional panels found to obtain number of two-dimensional panels	
:0	EPS ($\sim 10^{-4}\bar{c}$)	Maximum mismatch to be expected between three-dimensional panels	
:5	PANMX (50)	Maximum number of panels to be generated on a cross section	

CARD 15: Wake Streamline Description

Column	Variable	Description	Format
1-5	NSTN	Number of wake streamlines to be calculated	I5

CARD 16: Streamline Starting Points (Repeated NSTN times)

Column	Variable	Description	Format
1-10	XST	Starting x-value for streamline	3F10.0
11-20	(ISTDX)	Number of wake panel associated with wake streamline	
21-30	(DUBST)	Potential jump associated with wake streamline	

Note: ISTDX and DUBST should only be specified during a restart. They are normally left blank. This information is printed by the streamline tracker in the correct format for a restart.

END

FILMED

6-85

DTIC